Prog. Oceanog. 1983. Vol. 12, pp. 087–145.
Printed in Great Britain.

0079-6611/83/010087-59 $29.50/0

The Spatial and Temporal Development of the Spring Phytoplankton Bloom in the Celtic Sea, April 1979

M. J. R. FASHAM*, P. M. HOLLIGAN† and P. R. PUGH*

* *Institute of Oceanographic Sciences, Natural Environment Research Council, Wormley, Godalming, Surrey, U.K.*
† *Marine Biological Association, Plymouth, Devon, U.K.*

(*Received* 26 *October* 1982)

Abstract–The results are presented from three hydrographic surveys in April 1979 of a 40 × 50 km region of the Celtic Sea, centred at 7°W and 51°N, using a towed undulating sensor system. In the $5\frac{1}{2}$ days between Surveys 1 and 2, the seasonal thermocline was established, with surface to bottom temperature differences reaching 1.5°C, the average surface chlorophyll *a* level increased from ~ 1 to ~ 5.5 mg m^{-3} due mainly to the growth of diatoms, and the surface nitrate concentration decreased from 6 to 1 μM. The third survey was carried out after a further two days and, although surface properties changed little, there was a general deepening of the mixed layer due to stronger winds, and a further increase in the standing stock of phytoplankton.

By applying appropriate techniques of horizontal spatial averaging, which took into account possible advective effects, a quantitative comparison was made of the changes at two positions in the survey area which showed significant differences in the rate of development of the phytoplankton population. A simple model of phytoplankton growth was then developed, based on calculations of eddy diffusivity, on measurements of rates of photosynthetic carbon assimilation, and on observations of carbon to chlorophyll ratios, subsurface light attenuation and inorganic nutrient levels. In the absence of any data on zooplankton populations, the loss of phytoplankton by grazing was left as a free parameter.

The model was only partly successful in reproducing the observed changes in chlorophyll concentrations during the first $5\frac{1}{2}$ days and showed serious limitations for the subsequent 2 days. However, it emphasised several features of the dynamics of spring phytoplankton populations which require further experimental or observational investigation. These include more precise measurements of carbon to chlorophyll ratios and grazing pressure to which the model is sensitive over a rather narrow range (this has important implications in terms both of control by grazing and nutrient limitation), the potential significance of physiological photoadaptation by the plant cells in determining their vertical distribution, and the role of eddy diffusion across the developing thermocline in relation to the sinking of phytoplankton cells and the upward mixing of inorganic nutrients.

CONTENTS

1. INTRODUCTION

IN THE CELTIC SEA, the continental shelf region to the south west of the British Isles, the spring diatom bloom develops first in mid-April in the area to the south of Ireland where the tidal streams are relatively weak (PINGREE, HOLLIGAN, MARDELL and HEAD, 1976). The main increase in phytoplankton occurs as the seasonal thermocline is formed, with surface to bottom temperature differences $>0.2^{\circ}C$ sufficient to maintain favourable light conditions for plant cells in the surface layer through the inhibition of vertical mixing. The duration, as well as the intensity, of the bloom appear to be determined largely by prevailing weather conditions, with the depth of wind mixing and surface illumination being especially critical. However, the relative importance of biological properties, such as sinking and photoadaptation of the plant cells and grazing by herbivores, in determining the spatial and temporal distributions of the phytoplankton are not understood sufficiently well for predictions to be made about the effects of annual variations in the weather on production processes at this time of year. We have investigated some of these problems using data from the Celtic Sea in April 1979.

2. SURVEY METHODS AND INSTRUMENTATION

The survey area was situated to the south of the Nymphe Bank (Fig. 1). There is a general increase in the water depth over the area from the north to south-west, although in the north-east there is an area of deeper water representing the southern extremity of a trough in St. George's Channel. The detailed bathymetry (Fig. 2), derived from echo-sounder observations made on the cruise, agrees very well with that shown in Fig. 1. The edge of the trough can be seen on the south-eastern edge of the grid.

It was decided to survey a 40 x 50 km box, whose long axis was aligned with the major axis of the local tidal ellipse. This ellipse was determined from current meter data observed at

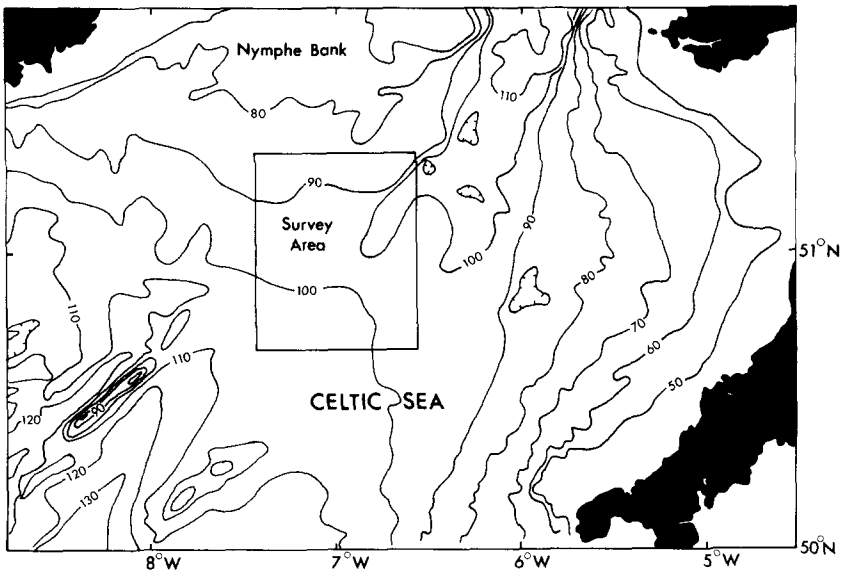

FIG. 1. Topographic chart of the northern Celtic Sea showing water depth (m) and the location of the survey area.

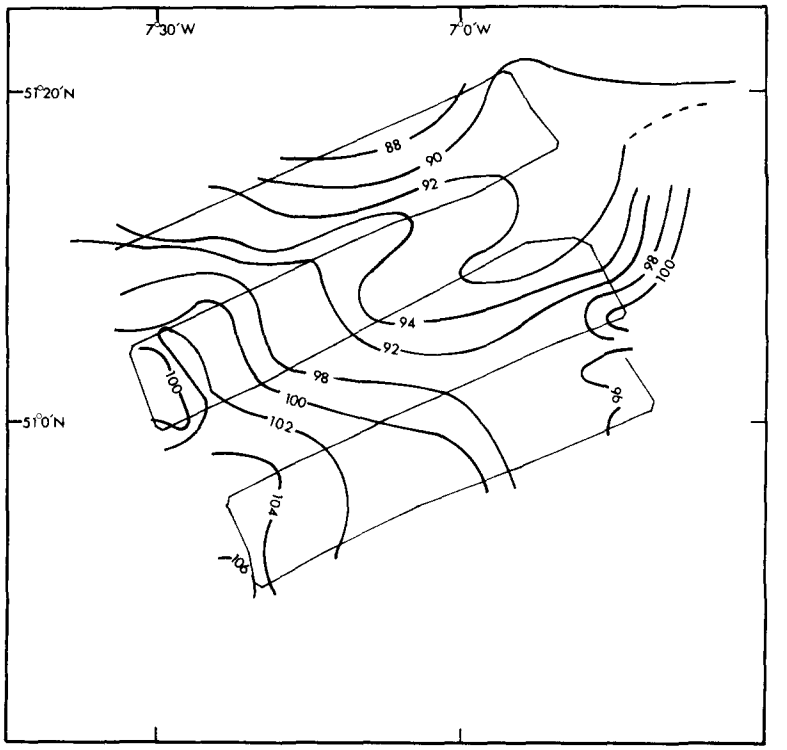

FIG. 2. Contours of water depth (m) in the survey area superimposed on the ship's track for Survey 1 (12–13 April).

station 010 by PINGREE, HOLLIGAN, MARDELL and HEAD (1976). The first survey was begun in the NW corner of the grid at 2220 hr on the 12th of April and ended in the SE corner at 1922 hr on the 13th. The second two surveys were started in the SW corner of the grid. Survey 2 was carried out between 2300 hr on the 18th of April and 2300 hr on the 19th, while Survey 3 was made exactly two days later. In between Surveys 1 and 2 the ship was working at the continental shelf break, some distance from the survey area.

Throughout the survey satellite navigation was used to fix the ship's position and the track was interpolated between fixes using ten minute values of gyrocompass and two-component electromagnetic log readings. In order to compare the results from the three surveys the interpolated ship's track was corrected for tidal motion. This was done using tidal constants derived for the area by the Bidston Laboratory of the Institute of Oceanographic Sciences (IOS), using information obtained from a mooring placed at 51°3′N, 7°0′W in June 1973. These data showed that the maximum tidal stream velocity at springs (April 13, 1979) was 40 cm sec^{-1}.

During the surveys information on the water column down to about 60 m was obtained using the IOS towed undulator, while data on the surface water were obtained by pumping water from the side of the ship and passing it through various continuously recording instruments on the ship. Figure 3 gives a schematic picture of the sampling devices and the data acquisition system.

The IOS undulator contained a Neil Brown Instrument System conductivity–temperature–depth probe (CTD) and was controlled by a Hermes servo-controller using the pressure signal from the CTD. The undulator was towed at an average speed of 7 knots, with an ascent/descent speed of about 1 m sec^{-1} and a cycle wavelength of about 0.4 km. The undulator was also fitted with a Chelsea Instruments Ltd. "Subaquatraka" fluorometer for measuring *in situ* chlorophyll concentrations (FASHAM, PUGH, GRIFFITHS and WHEATON, 1981).

Surface sea water was sampled, at a rate of 150 ℓ min^{-1}, with a submersible pump attached to the ship's side 2 m below the waterline. Most of this water was supplied via a header tank to a Plessey Thermosalinograph, with the remainder passing directly into the laboratory both to a Turner Model III fluorometer for measurements of chlorophyll *a* fluorescence and to a nutrient autoanalyser. The latter measured the concentration of nitrate (STRICKLAND and PARSONS, 1968), nitrite, ammonium and silicate ions although only the nitrate results will be discussed in this paper. The surface water temperature was also recorded by an IOS fast response temperature probe towed from the after quarter of the ship.

For vertical profiles on station the CTD and Chelsea fluorometer were removed from the undulator and attached, together with a Plessey irradiance meter, to the hydrographic wire. A length of plastic hosing (5 cm internal diameter) was attached to the CTD frame and water was supplied by a second submersible pump to the laboratory instruments to give vertical profiles of nutrients as well as comparative profiles of chlorophyll *a* fluorescence with the Turner fluorometer. These observations were made at six stations, one at the NW corner of the grid at the end of Survey 1 and five between Surveys 2 and 3 at the western end of each long leg (see Fig. 9).

The Plessey underwater irradiance meter has been described by KAHN, PUGH, FASHAM and HARRIS (1975). A temperature compensated silicon photodiode is used to measure radiation and the input colour filter has been chosen to give a virtually flat energy response over the photosynthetic wavelength range from 350 to 700 nm. The output from the photodiode was amplified and converted to give an output proportional to the logarithm of the irradiance. The meter was calibrated in air using an He–Ne laser and a set of precision attenuators, and this calibration was adjusted for the water immersion effect using the data of SMITH (1969).

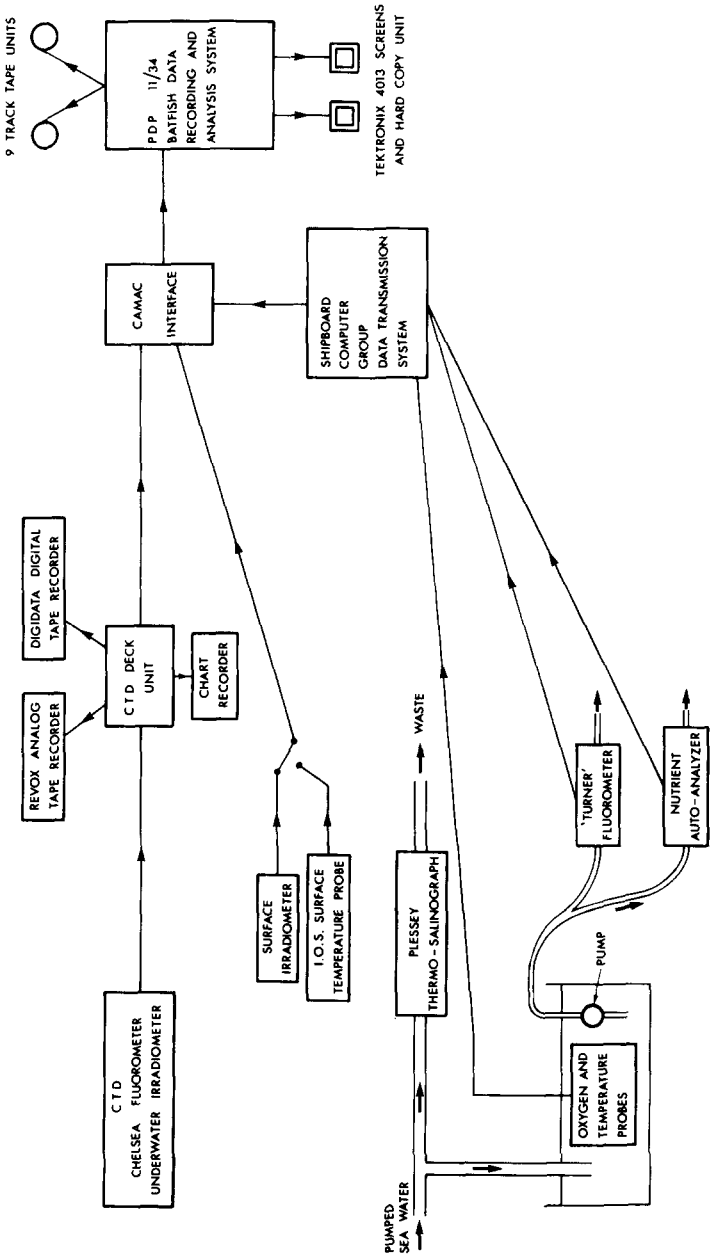

FIG. 3. Diagram of the water sampling and data acquisition systems (for further details, see text).

Throughout the cruise incident photosynthetic irradiance (350–700 nm) was recorded using a Lambda Quantum Meter, and wet and dry air temperature, wind speed and air pressure were recorded manually at four hourly intervals from standard ship's instruments.

The CTD and fluorometer were all sampled at 16 Hz, digitised and telemetered from the undulator to the CTD deck unit, where it was decoded and stored on a digital 9 track and analogue tape recorder, the latter being a back-up facility. These data, together with 1 second samples from the surface temperature probe, were also sampled by a PDP11/34 computer which enabled a certain amount of data analysis and display to be carried out at sea. The data from the Turner fluorometer, autoanalyser and thermosalinograph were recorded on chart recorders.

Water samples for determinations of plant pigments, particulate carbon and nitrogen, and for phytoplankton counts were collected from the outflow of the Turner fluorometer. Chlorophyll *a* and phaeopigments were estimated for a total of 172 samples by filtering 25–200 ml of water on GF/C filters, and measuring the fluorescence of 90% acetone extracts before and after the addition of acid (HOLM-HANSEN, LORENZEN, HOLMES and STRICKLAND, 1965). Samples for total particulate organic C and N were collected on combusted glass fibre filters and analysed on a Carlo Erba Elemental Analyser. The phytoplankton was preserved for Lugols iodine, and cell counts made on an inverted microscope. Cell volumes were calculated for each of the dominant species (see Table 1) by direct measurements of the dimensions of 50–100 cells, and converted to phytoplankton carbon using the cell volume/carbon relationships derived by EPPLEY, REID and STRICKLAND (1970).

Rates of photosynthetic carbon fixation were measured by incubating 130 mℓ samples of surface sea water, after the addition of 5 μCi $NaH^{14}CO_3$, in a deck incubator at light intensities corresponding to 100, 60, 40, 9 and 0% of surface irradiance. After 2.5–3.5 hr the samples were filtered on to 0.45 μm membrane filters and radioactivity in the particulate material assayed as described by PINGREE, HOLLIGAN, MARDELL and HEAD (1976). The counts were converted to mg C fixed [mg chlorophyll $a]^{-1}hr^{-1}$, using the mean of chlorophyll *a* concentrations at the start and end of the incubation period. The concentration of dissolved inorganic C was assumed to have been 2.0 mM; this may have led to a slight overestimation of rates of carbon fixation if the pH of the sea water increased during the development of the bloom (see WEICHART, 1970).

3. CALIBRATION AND DATA REDUCTION

The temperature sensors in the CTD and surface temperature probe were calibrated in the laboratory using a platinum resistance transfer standard. The thermosalinograph temperature sensor was calibrated on the ship using reversing thermometers, while the salinity sensor was calibrated against a Guildline salinometer.

The calibration of the conductivity sensor in the undulator presented some problems. It is possible to obtain an initial calibration by taking water bottle samples close to the sensor and then measuring the conductivity of the samples in the usual way. However, conductivity cells are often known to exhibit calibration drift due to the accumulation of deposits on the cell, and to also make sudden jumps caused by fouling of the cell. These changes are often temporary but may last a few hours. For long undulator runs it was therefore necessary to devise a method of calibrating the conductivity sensor *in situ*. From a knowledge of the ship's speed, the undulator cycle time and the transit time of water in the pump system, it was possible to calculate

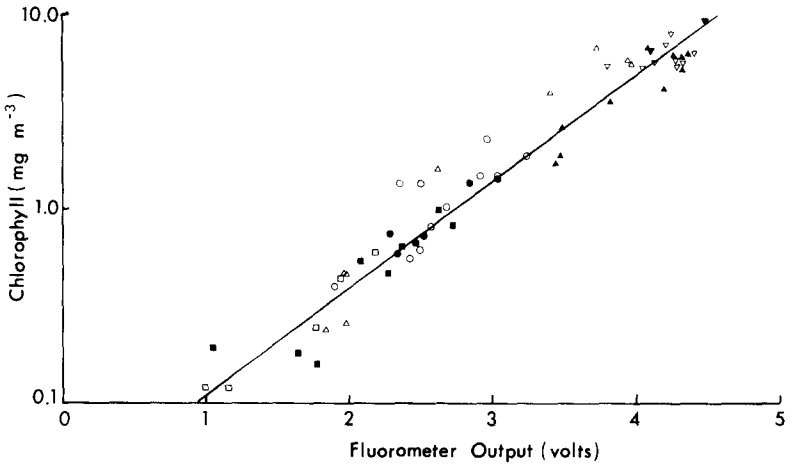

FIG. 4. Calibration of the Chelsea fluorometer. Regression analysis gives the equation for all data points.
The symbols correspond to the following data groups. Squares – Shelf edge survey, circles – Survey 1, triangles – Survey 2, inverted triangles – Survey 3. Day samples are open and night samples closed symbols.

the time at which to take a water sample on the ship, which corresponded to the surface water samples by the undulator. Obviously errors can arise from this method if used in regions of strong horizontal gradients or if the undulator did not penetrate the surface mixed layer. However, such points can be excluded from the calibration process.

The Chelsea fluorometer was calibrated partly by using this method and partly with samples taken on the vertical profiles. The fluorescence yield (the ratio of chlorophyll *a* fluorescence intensity to chlorophyll *a* concentration) of a natural assemblage of phytoplankton can vary with species composition (STRICKLAND, 1968; SLOVACEK and HANNAN, 1977) and with the physiological state of the plant cells (KIEFER, 1973; CULLEN and RENGER, 1979) and it is thus necessary to calibrate frequently. During the course of the cruise, 60 calibration samples were obtained for the Chelsea fluorometer. The results (Fig. 4) have been divided into eight groups based on different time periods of the cruise and whether the calibration was made during the day or night.

A linear calibration line has been fitted to all the data using the major axis regression method (YORKE, 1966) as both x and y variables are subject to error. The majority of the readings from Surveys 2 and 3 had higher chlorophyll values than those from Survey 1 and the shelf edge survey, but despite this change the regression line gives a good fit to the data throughout the whole chlorophyll range. Furthermore, there is no evidence for a significant change of calibration during the duration of the cruise. This contention is supported by the fact that the low chlorophyll samples from Survey 2, which were obtained from deep bottle samples, straddle the regression line. There is some evidence of a day to night change in fluorescence yield particularly for Survey 2. All the day-time samples from this survey lie above the regression line while the night-time samples lie on or below the line. This result is consistent with the fluoresence yield being reduced during the day-time when active photosynthesis is taking place (KIEFER, 1973; CULLEN and RENGER, 1979). However, the data from the other three periods did not show such consistent behaviour and so the combined day and night data were used to calculate the calibration curve.

Some data reduction and plotting was carried out at sea on the PDP11/34 in order to aid the day-to-day planning. However, the final analysis was done in the laboratory when the calibration data were available using the G-EXEC software package (JEFFREY, GILL, POLLARD and COLLINS, 1977). The 16 Hz CTD pressure, temperature and fluorescence readings were first averaged to give half-second values and then calibrated. The determination of the conductivity averages presented some problems due to the mismatch in time constant between the temperature and conductivity sensors which produced salinity spikes in areas of high temperature gradient. This problem has been discussed fully by MILLARD, TOOLE and SWARTZ (1980), and POLLARD (1980) whose digital filter was applied to the conductivity readings before averaging. The half-second values of temperature, pressure and conductivity were then used to calculate salinity and density σ_t. The calibrated half-second undulator data were finally merged with the navigation data, interpolated from the ten minute values of tidally corrected ship's position.

To portray the three-dimensional structure of the hydrographic properties the results of the surveys will be presented either as horizontal contoured sections of the surface data and undulator data for 47.5 m (this depth was chosen as being the deepest depth sampled consistently by the undulator on all three surveys) or as vertical contoured sections of the undulator data. Values from the undulator sections were taken only from the down traces. The main reason for this was that the one second response time of the Chelsea *in situ* fluorometer meant that down and up chlorophyll traces could show relative displacements of up to 2 m in the chlorocline. Thus if both down and up traces were used spurious horizontal variability may be introduced into the contoured sections. The down traces were chosen because the salinity spiking referred to earlier was less intense than on the up traces (POLLARD, 1980). The horizontal sections were contoured by hand while the vertical sections were contoured using the SURFACE II program (SAMPSON, 1978).

4. RESULTS

4.1. *Meteorological observations*

The observations of wind speed and direction obtained on the cruise are shown in Fig. 5. Between the first and second surveys the ship was on passage to and from the shelf edge, but data from meteorological stations surrounding the Celtic Sea all show very similar trends. At the start of Survey 1 the wind was around 20 knots from the south but during this survey and the first part of Survey 2 the barometric pressure rose steadily with a consequent drop in wind speed to less than 10 knots. On the 18th April the pressure began falling and the wind increased to 20 knots by the middle of Survey 2, thereafter remaining between 10 and 20 knots mainly from the west. Calculations from observations of total solar radiation obtained from the Aberporth Observatory in SW Wales (Fig. 5) showed that the cloud cover for the period was generally between 5% and 15%, with the exception of the 13th and 19th of April when values of 55% and 75% were observed.

4.2. *Undulator and surface water observations*

As space does not allow vertical sections for all the legs of each survey to be displayed a selection has been made to illustrate important features of the observed temporal and spatial

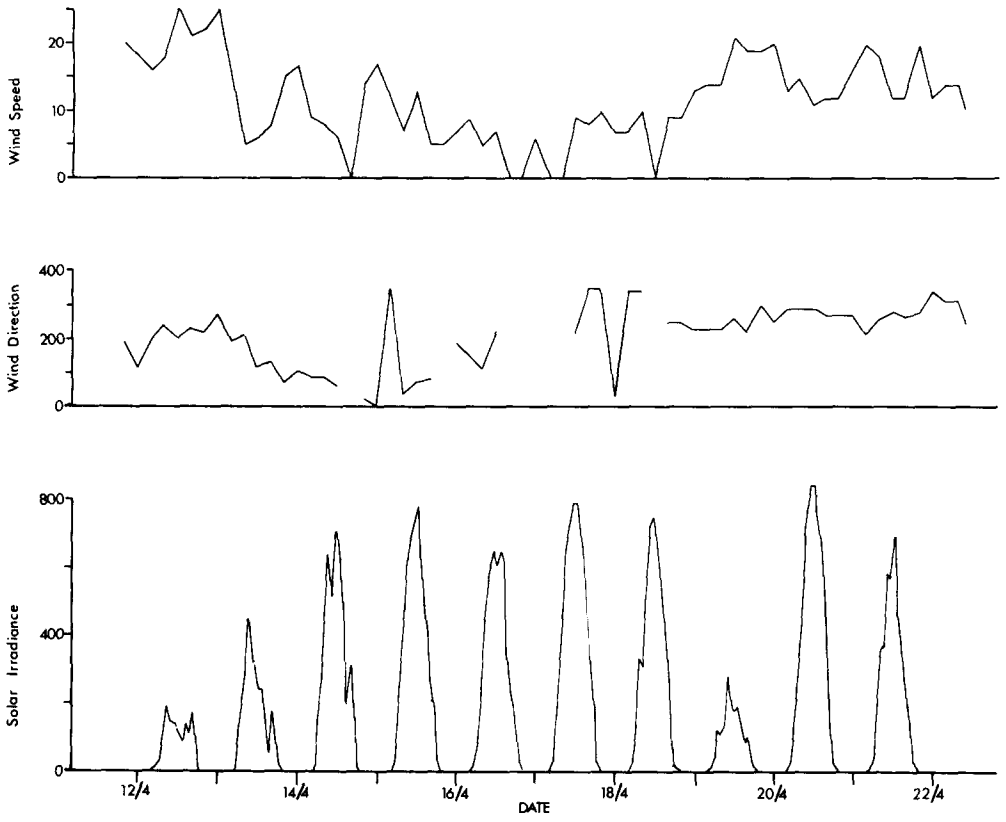

FIG. 5. Summary of ship observations on (a) wind speed (knots); (b) wind direction (degrees); (c) solar irradiance (watts m^{-2}) for the period 12–22 April, 1979. Note that on the 14–18 April work was being carried out along the shelf break, well to the south west of the survey area.

changes. It should also be emphasised that the surveys were not synoptic so that the hoizontal and vertical sections are based on data collected over 24 and 6 hr respectively.

4.2.1. *Survey 1.* Contours of the horizontal distribution of temperature, salinity, chlorophyll and nitrate in the surface water and temperature and salinity at a depth of 47.5 m are shown in Fig. 6 (a–f). The leg numbers referred to in the text are indicated on Fig. 6(b). The temperature contours at the surface [Fig. 6(c)] and at 47.5 m [Fig. 6(e)] showed a similar pattern, with colder water in the NE and warmer water in the SW. A comparison with Fig. 2 shows that this trend was closely correlated with water depth, as would be expected at the end of the winter cooling period (BOWDEN, 1955). The other feature of the temperature field was a zone of high horizontal gradient running in a NW to SE direction between, at the surface, the 8.0°C and 8.6°C isotherms. This high gradient zone (HGZ) separated an area of intermediate horizontal gradients in the SW from an area in the NE where the gradients were weak. The distribution of surface chlorophyll [Fig.6(a)] was related to the HGZ; to the SW of it the chlorophyll values were less than 1 mg m^{-3}, while to the NE values of up to 2 mg m^{-3} were found. The surface nitrate values [Fig. 6(b)] also showed a SW to NE trend, but with the lower levels correlated to high salinity and temperature rather than to high chlorophyll.

The vertical section for Leg 9 (Fig. 7) shows that the HGZ, as defined by the 7.8°C and

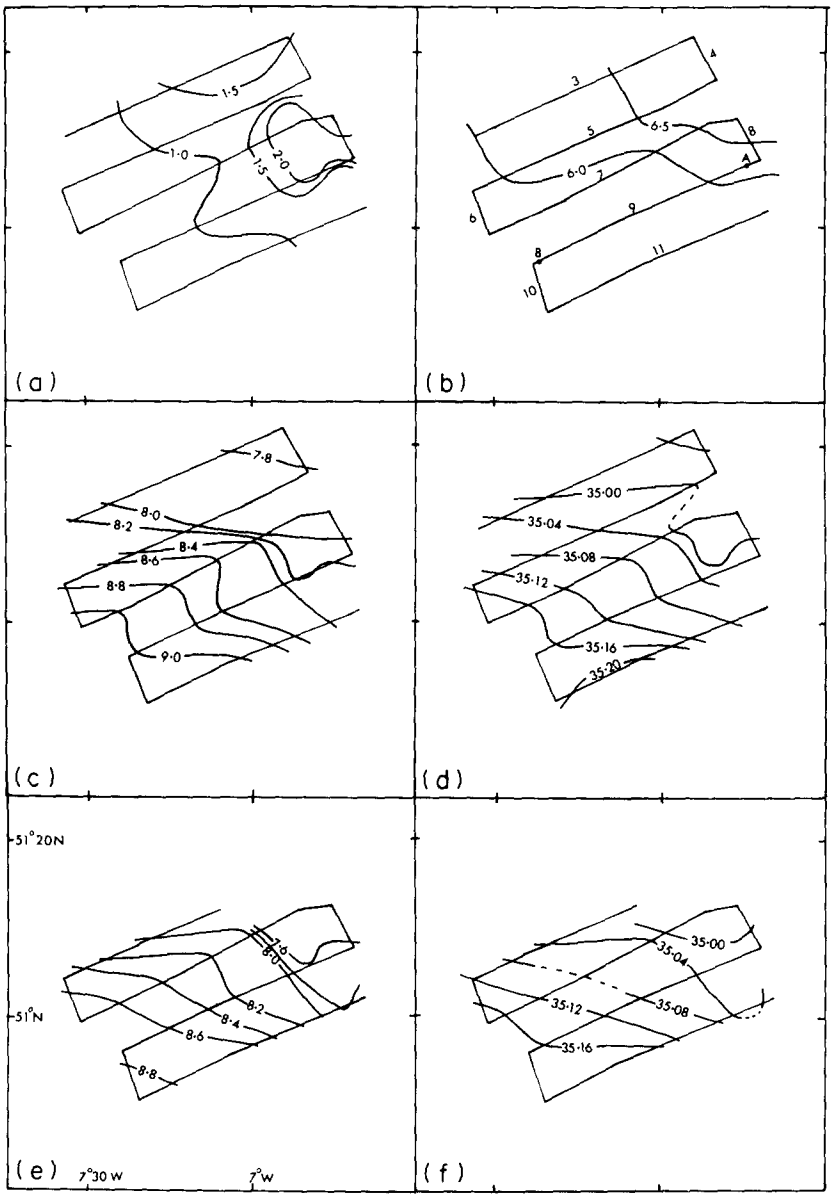

FIG. 6. Survey 1, 2220 hr April 12–1922 hr April 13, (a) to (d) observations at 2 m (surface), (e) and (f) observations at 47.5 m –

(a) chlorophyll *a* (mg m^{-3});
(b) nitrate (μM), and also leg numbers for Survey 1 and positions of A and B (see Section 5.1);
(c), (e) temperature (°C);
(d), (f) salinity ($^0/_{00}$).

8.0°C isotherms, extends from the surface to at least 60 m. These isotherms dip down at an angle of about 2° to the horizontal. The most striking feature of the temperature sections was the difference in vertical stratification on either side of the HGZ. Throughout the whole section

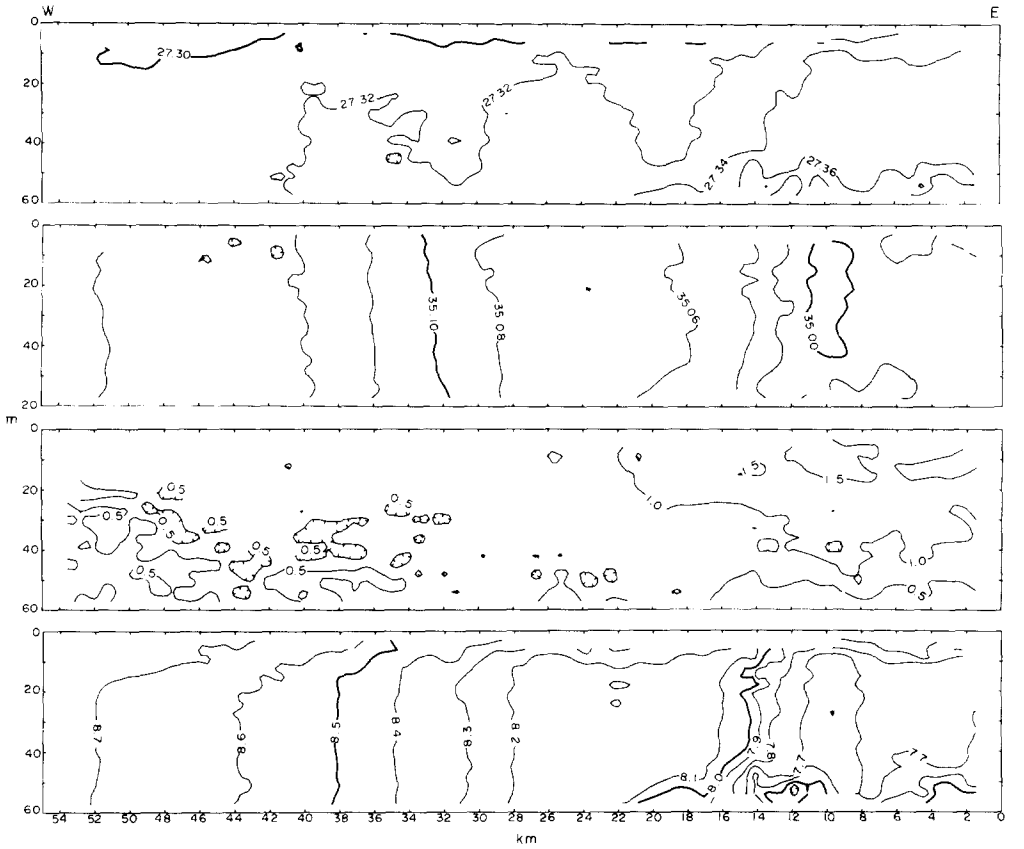

FIG. 7. Survey 1, Leg 9, vertical distributions of (a) density (σ_t units); (b) salinity (‰); (c) chlorophyll *a* (mg m^{-3}); (d) temperature (°C).

there was a shallow thermocline between 5 and 10 m with a temperature difference between the surface and 20 m of about 0.1°C. To the east of the HGZ there was also a deep thermocline between 45 and 55 m resulting in a total top-to-bottom temperature difference of around 0.4°C. In between the two thermoclines the water was virtually isothermal. Unfortunately on this leg the undulator did not penetrate deep enough to be certain that the water below this deep thermocline was well mixed. However, other data obtained in this area at this time of year (JAMES, 1980) suggest that this was the case. The deep thermocline extended for a short distance to the west of the HGZ.

The salinity section showed the same pattern of horizontal gradients as the temperature data but no vertical structure. In the area of the HGZ and to the NE, the density field was mainly determined by temperature as shown by the similarities of the temperature and σ_t sections. To the SW of the HGZ, however, temperature and salinity were self-compensating and there was virtually no horizontal gradient of density. The dynamic implications of the horizontal change in density across the HGZ, which are discussed more fully in Section 5.1, would imply a geostrophic south-easterly trending current in the HGZ. The density was clearly defined on Legs 3, 7 and 11, as well as 9, and in all cases coincided with the temperature HGZ. Thus the horizontal

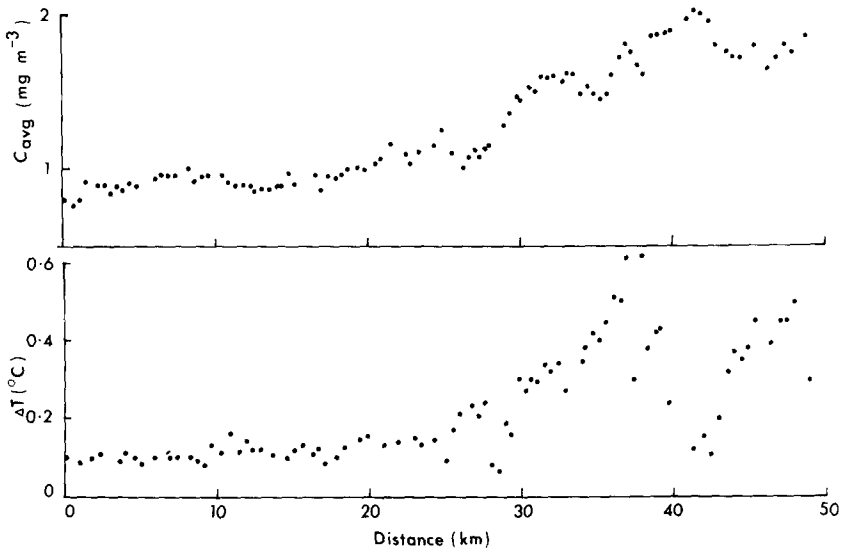

FIG. 8. Survey 1, Leg 9. Changes from west to east in (a) depth averaged chlorophyll *a* concentration (mg m^{-3}) for each undulation; (b) temperature difference (°C) between top and bottom of each undulation. For further details of vertical distributions, see Fig. 7.

maps of temperature [Figs 6(c), 6(e)] can be used to trace the direction of this current which veered from easterly to south-easterly as it crossed the survey area.

The chlorophyll section shows that the horizontal and vertical distribution of the phytoplankton was correlated with the changes in stratification on either side of the HGZ. To the east of this zone values in excess of 1 mg m^{-3} chlorophyll *a* were found as far down as the deep thermocline, while to the west the concentration was generally less than 1 mg m^{-3}. It is worth emphasising that the horizontal gradients of chlorophyll in the HGZ were not as strong as those for temperature or density. It is probable that the relatively high chlorophyll levels to the west of the HGZ were due to the extension westwards of the deep thermocline referred to earlier. This supposition is supported by comparing a plot of the temperature difference between the top and bottom of the undulator cycle and the depth averaged chlorophyll concentration for that cycle (Fig. 8). The undulator did not always reach the same maximum or minimum depths and so there is a certain amount of noise in these values. However, it is clear that the average chlorophyll value is correlated with the temperature difference and that the average chlorophyll began to increase at a point where the temperature difference exceeded 0.2°C.

One vertical profile of nitrate distribution was obtained at the end of Survey 1 in the NW corner. This showed that the nitrate concentration was virtually constant between the surface and 70 m.

4.2.2. *Survey 2.* The second survey was begun six days after the first, although for logistic reasons it was started in the SW rather than NW corner of the survey box. The time difference between comparable legs of the two surveys was therefore not constant, being for example 5½ days between Legs 9 and 34 and 7 days between Legs 3 and 40. The horizontal contoured sections for Survey 2 are shown in Figs 9 (a–f).

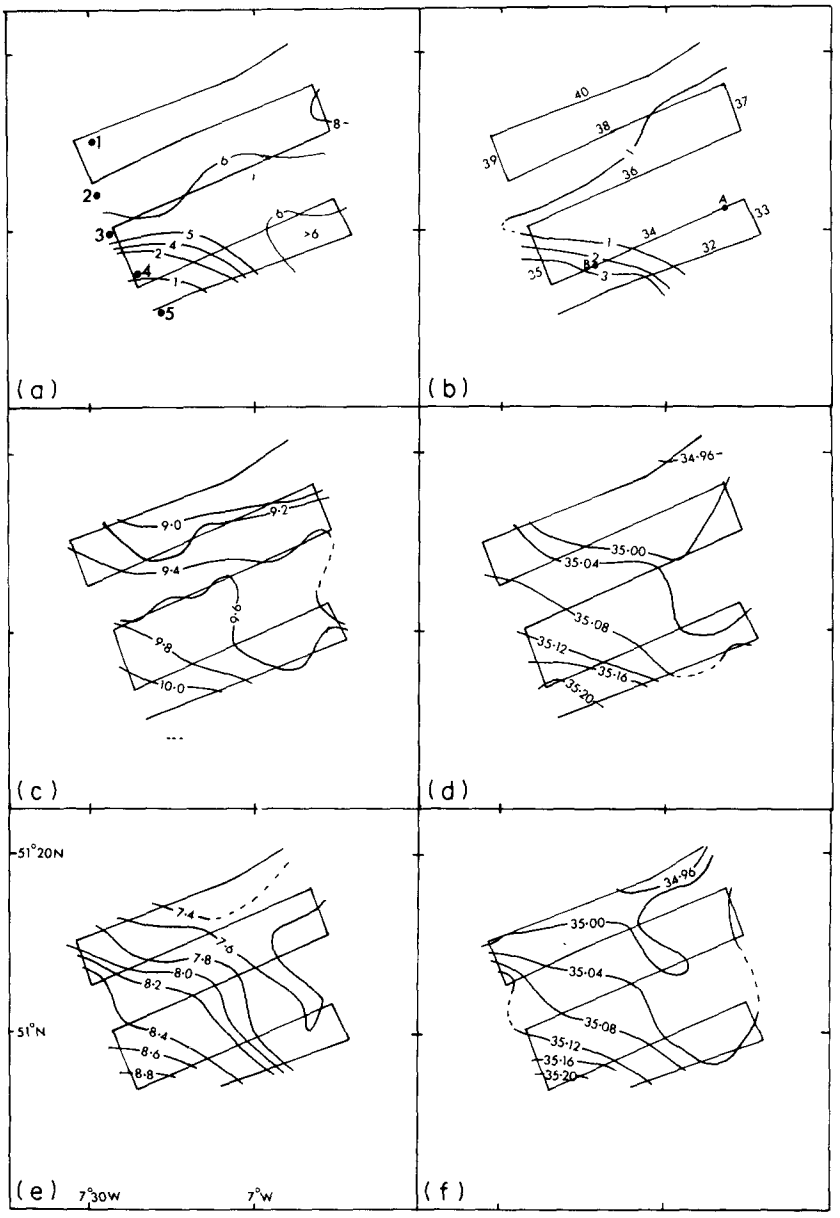

FIG. 9. Survey 2, 2300 hr April 18–2300 hr April 19, (a) to (d) observations at 2 m (surface), (e) and (f) observations at 47.5 m –
(a) chlorophyll *a* (mg m^{-3}) and positions of vertical profiles.
(b) nitrate (μM) and also leg numbers for Survey 2 and positions of A and B.
(c), (e) temperature (°C);
(d), (f) salinity (‰).

A comparison of Figs. 6(e) and 9(e) shows that between Surveys 1 and 2 there was very little change in the temperature at 47.5 m implying that there had been little penetration of surface heating to this depth. The HGZ was still clearly defined, spanning a temperature range from

7.8°C to 8.2°C compared with a range of 7.6°C to 8.0°C on Survey 1. The salinity distributions for the two surveys were also similar [Figs 9(d), 9(f)], implying that there were no advective changes on a scale larger than the survey area between Surveys 1 and 2. By contrast, the temperature of the surface water had become at least a degree warmer in the intervening period and showed complex horizontal structures. There were apparent areal differences in the amount of heat absorbed by the water column as the maximum horizontal temperature difference across the survey area was reduced from between 1.4°C–1.5°C on Survey 1 to 1.2°C on Survey 2. Possible reasons for this will be given in Section 5.3.

The surface chlorophyll values [Fig. 9(a)] showed a four to five-fold increase over most of the survey area since Survey 1, with the highest values again observed in the NE. In the SW corner, however, the chlorophyll concentration remained less than 1 mg m^{-3}. It is difficult to estimate the phytoplankton increase in the SW as the steep horizontal gradients make matching of the distributions from the two surveys very difficult. However, a technique for dealing with this problem, presented in a subsequent section, indicates that in the SW the chlorophyll increased by a factor of about 2 between Surveys 1 and 2. A comparison of the surface chlorophyll and the temperature at 47.5 m [Figs 9(a), 9(e)] shows that the boundary between the zones of high and low chlorophyll was still correlated with the HGZ, although due to the effect of surface heating this would not be apparent from surface observations alone. It should be emphasised that the horizontal differences in chlorophyll observed along, say, Legs 32 or 34 are too great to be attributed to temporal changes occurring within the time scale of the second survey. If we take the figure of a five-fold increase in chlorophyll in 6 days this would only mean an increase of 5% during the time taken to traverse one leg.

The surface nitrate concentrations [Fig. 9(b)] had decreased to ~1 μM except in the SW corner, showing an inverse correlation with the chlorophyll.

The contoured sections for Leg 34, which was closest to Leg 9 of Survey 1, are shown in Fig. 10. A shallow thermocline had developed throughout the whole leg, while below 10 m there was a more gradual temperature decrease down to about 50 m in the east or 30 m in the west. Below the shallow thermocline the HGZ could still be distinguished between the 7.6°C and 8.2°C isotherms. The density section was very similar to temperature except for the area to the west of the HGZ where, as on Survey 1, the horizontal gradients of temperature and salinity were self compensating.

The depth to the bottom of the shallow thermocline varied on Survey 2 from 10 m on Legs 32 to 36 to about 25 m on Legs 38 to 40. This deepening of the surface mixed layer was probably caused by the increase in wind speed during the survey (Fig. 5), a contention supported by the results of Survey 3 which showed the bottom of the thermocline to be at ~ 25 m throughout the whole area. This is an example of a situation when the time scale of the processes being studied was of the same order as the time scale of the survey and emphasises the care needed in interpretating such data.

The chlorophyll section shows that most of the phytoplankton increase took place in the surface 20 m. The chlorocline extended from around 10 m down to 30 m, below which the chlorophyll concentration was less than 1 mg m^{-3}. Thus in the period before the increase in wind strength, the base of the main thermocline (between 5 and 10 m) coincided approximately with the top of the chlorocline. By contrast, with the increase in wind strength from Leg 37 onwards and throughout Survey 3 the chlorocline and thermocline were at the same depth.

Another striking feature of the chlorophyll data is that, despite the development of a thermocline throughout the whole leg, there was still a pronounced horizontal gradient of chlorophyll which was, as on Survey 1, correlated with the difference in temperature across

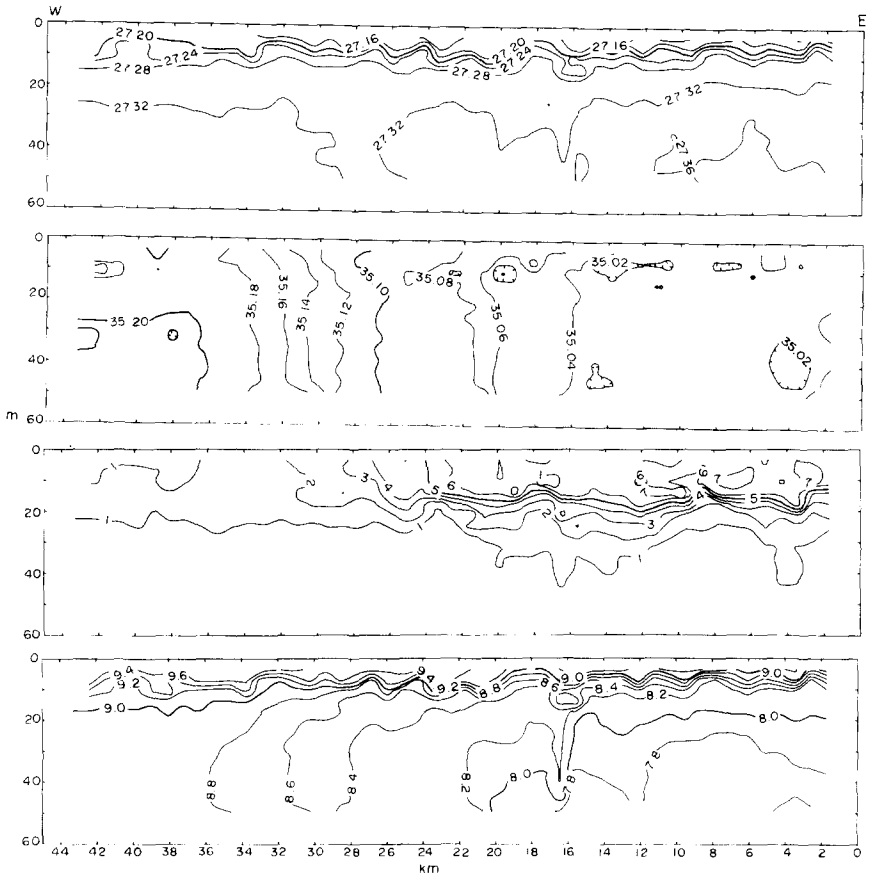

FIG. 10. Survey 2, Leg 34. Vertical distributions of (a) density (σ_t units); (b) salinity (‰); chlorophyll *a* (mg m^{-3}); (d) temperature (°C).

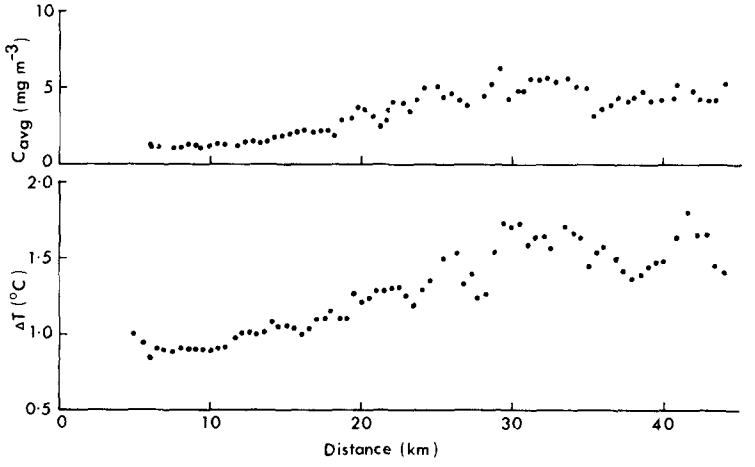

FIG. 11. Survey 2, Leg 34. Changes from west to east in (a) depth averaged chlorophyll *a* concentration (mg m^{-3}) for each undulation; (b) temperature difference (°C) between top and bottom of each undulation. For further details of vertical distributions, see Fig. 10.

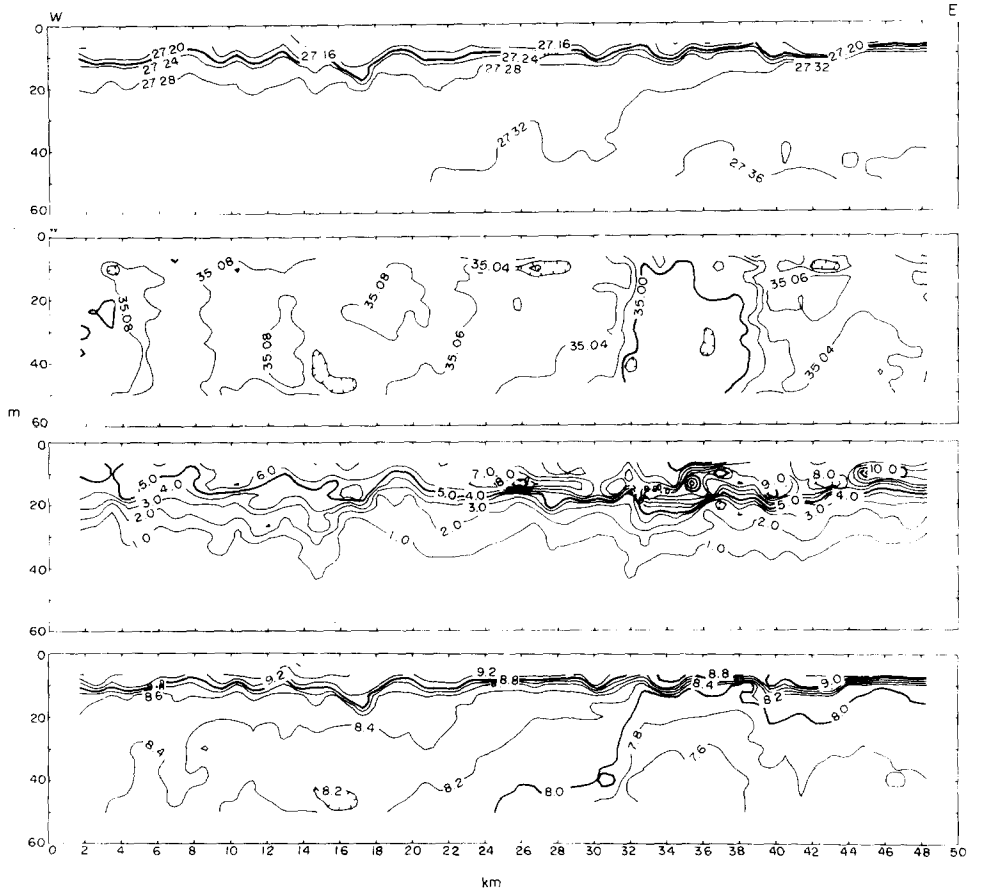

FIG. 12. Survey 2, Leg 36. Vertical distributions of (a) density (σ_t units); (b) salinity (‰); (c) chlorophyll *a* (mg m^{-3}); (d) temperature (°C).

the thermocline (Fig. 11). This suggests that the changes in chlorophyll observed along Leg 34 were due, at least in part, to a temporal lag in the development of stratification in the SW part of the survey area which in turn delayed the development of the phytoplankton population.

The contoured data for Leg 36 (Fig. 12) show the appearance, in the eastern half of the sections, of a sub-surface chlorophyll maximum just above the chlorocline. These peaks, which can be traced for distances of up to 1.5 km, reached values of up to 11 mg m^{-3}. Similar features were observed on Legs 38 and 40 although they were most strongly developed on Leg 36.

The change in the vertical distribution of nitrate between the high and low chlorophyll areas is seen in the north–south section obtained from the vertical dips made at the end of Survey 2 (Fig. 13). The thermocline was at a depth of ~ 20 m throughout the section but was weaker in the south. The chlorophyll in the south was less than 2 mg m^{-3} at the surface while in the north there was a sub-surface maximum of 6 mg m^{-3}. Below the chlorocline the nitrate concentration had decreased by about 1 μM from Survey 1 while at the surface it had decreased by 3–4 μM in the SW and 5 μM in the NE.

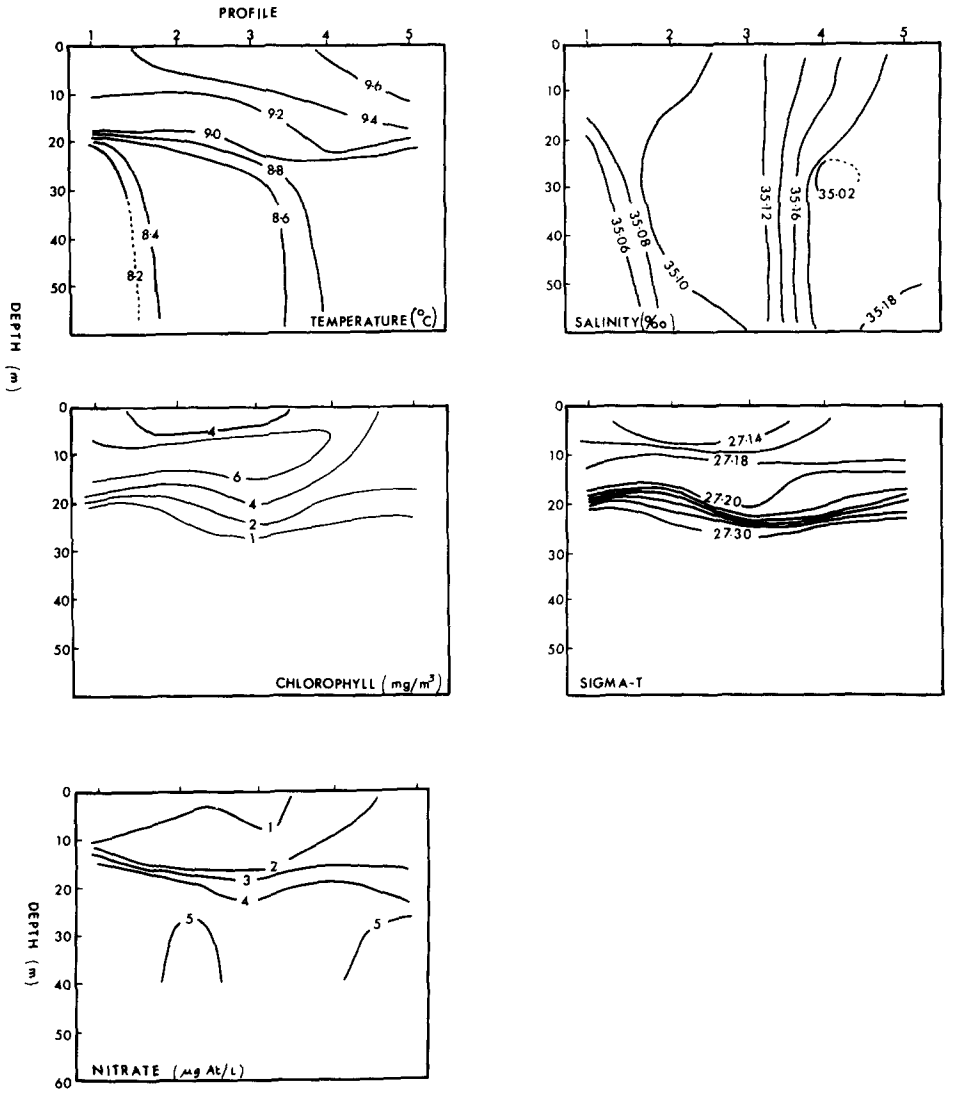

FIG. 13. Vertical distributions of (a) temperature (°C); (b) salinity (‰); (c) chlorophyll *a* (mg m^{-3}); (d) density (σ_t units); (e) nitrate (μM) on 20 April along western edge of survey area – see Fig. 9.

4.2.3. *Survey 3.* Survey 3 was carried out two days after Survey 2 and during the intervening period the wind speed, which had begun to increase half way through Survey 2, remained in the range 10 to 20 knots. The plot of surface temperature [Fig. 14(c)] shows that the resultant increased mixing had the effect of lowering the surface temperature. There was also a further reduction in the overall horizontal temperature gradient to less than 0.7°C. However, distribution of temperature at 47.5 m [Fig. 14(e)] and the salinity data (surface and 47.5 m) remained very similar from all three surveys.

The surface chlorophyll and nitrate distribution [Figs 14(a, b)] still showed the spatial variations observed on the two previous surveys. However, in the SW there were now no chlorophyll

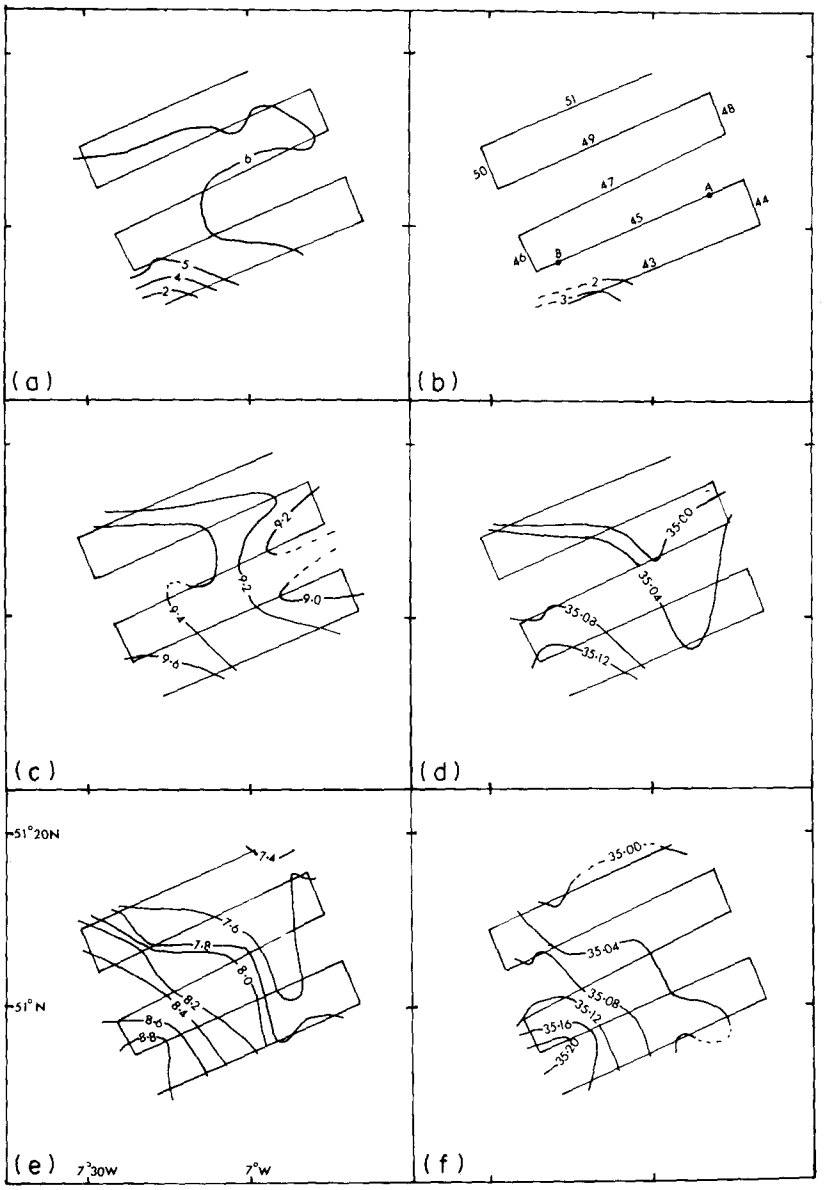

FIG. 14. Survey 3, 2300 hr April 20–2300 hr April 21 (1) to (d) observations at 2 m (surface), (e) and (f) observations at 47.5 m

(a) chlorophyll *a* (mg m^{-3});
(b) nitrate (μM), and also leg numbers for Survey 3 and positions of A and B;
(c), (e) temperature (°C);
(d), (f) salinity (‰).

values less than 1 mg m^{-3} and the area with low chlorophyll and high nitrate had contracted. Over the remainder of the survey area the values for chlorophyll and nitrate were similar to those found on Survey 2. The chlorophyll concentration to the north and west of the 6 mg m^{-3} contour reached values up to 8 mg m^{-3} but the patchy distribution made contouring in this area difficult.

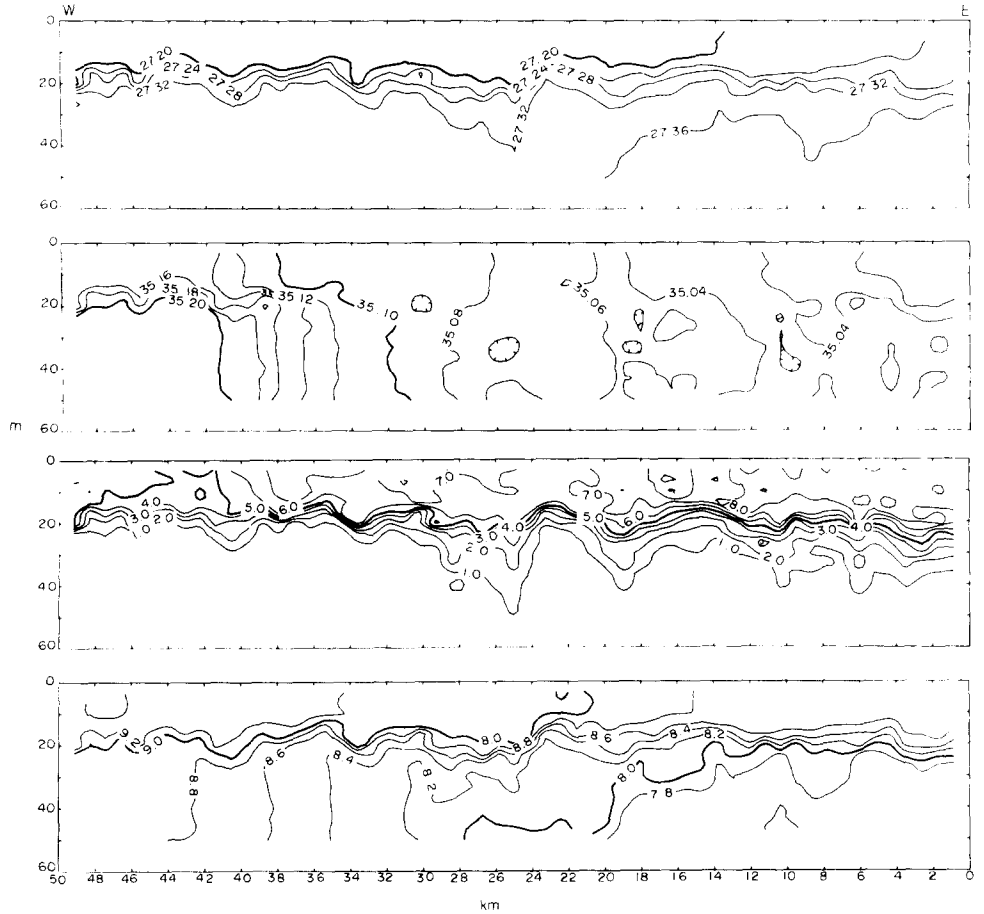

FIG. 15. Survey 3, Leg 45. Vertical distributions of (a) density (σ_t units); (b) salinity (‰); (c) chlorophyll *a* (mg m^{-3}); (d) temperature (°C).

The contoured sections for Leg 45, the equivalent of Legs 9 and 34, are shown in Fig. 15. Both the thermocline and pycnocline extended from a depth of 15 m to 25 m below the surface above which the water was well mixed. Below the thermocline the horizontal pattern was similar to Leg 34. The salinity data showed the development, at the western end, of a pronounced halocline while at the eastern end there was a small reversed halocline with more saline water overlaying less saline. Considering the timescale the most probable explanation for the development of these haloclines would be the vertical shear of the waters above the pycnocline relative to those beneath. In the case of the western end of the leg this would imply that the surface waters moved in a westerly to south-westerly direction, conforming with the wind direction during this period. If it is assumed that the halocline was produced solely by wind-induced shear, then by matching up the salinity contours in the SW corner of Figs 14(d) and (f) the relative movement of the water above and below the thermocline can be deduced. This yields a wind-induced surface water velocity of ~ 5 cm sec^{-1} which is consistent with wind speeds in the range 10 to 20 knots. The development of this halocline had the effect of sharpening the pycnocline so that the vertical gradient of density was now greater in the west than the east, the reverse of the situation on Survey 2.

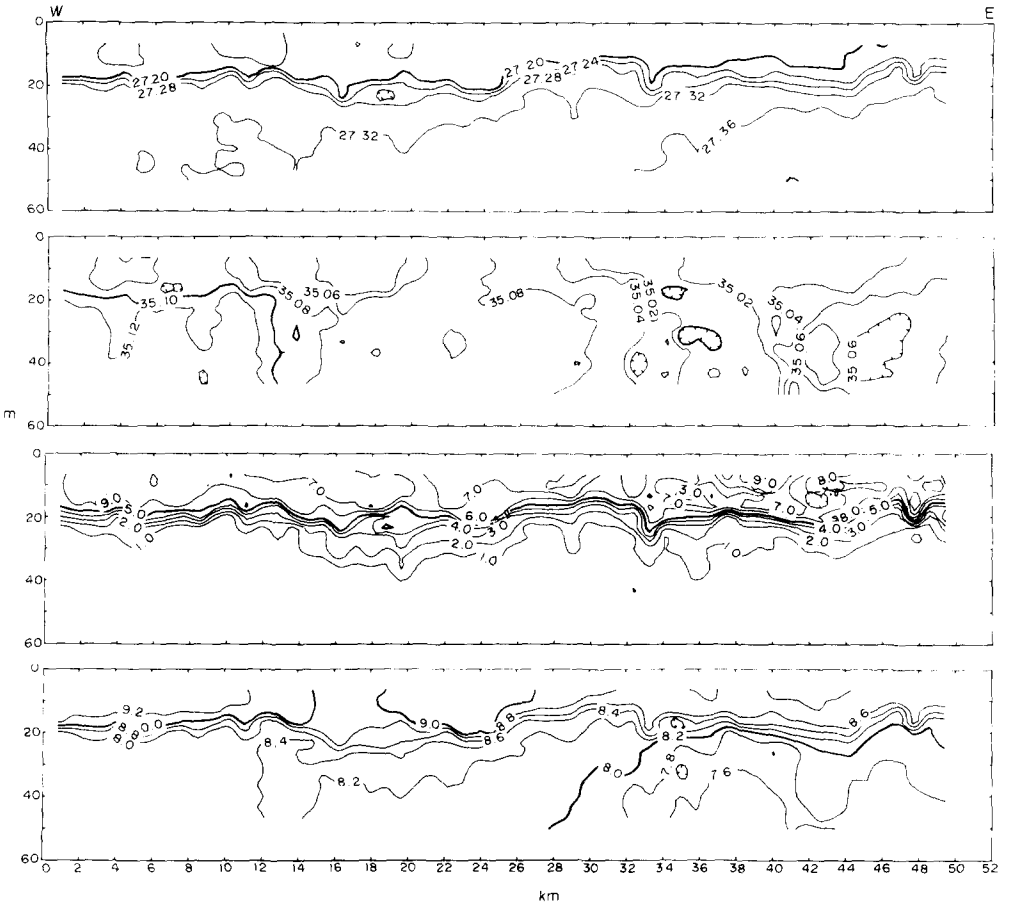

FIG. 16. Survey 3, Leg 47. Vertical distributions of (a) density (σ_t units); (b) salinity (‰); (c) chlorophyll *a* (mg m^{-3}); (d) temperature (°C).

The chlorophyll concentration at the east end of Leg 45 had reached maximum values of 9 mg m^{-3} compared with 6 mg m^{-3} on Survey 2. The top of the chlorocline on this leg was ~ 15 m, about 5 m deeper than on Survey 2, and the same depth as the top of the thermocline. Thus the effect of the wind mixing had been to mix both temperature and chlorophyll down to 15 m so that the vertical gradients of the two quantities had become coincident. At the western end of the leg chlorophyll had increased from 1–2 mg m^{-3} on Survey 2 to 5–6 mg m^{-3} suggesting that the phytoplankton population in the west was growing faster than that in the east, thus reducing the east–west gradient. The wind-induced SW movement of the surface waters referred to above could also have contributed to this effect.

The data for Leg 47 (Fig. 16) also showed a sharpening of the chlorocline and development of a halocline at the western end. However, it is interesting to note, that, at the eastern end, the sub-surface chlorophyll maxima noted on Leg 36 were still present. In Fig. 17 typical vertical profiles of temperature and chlorophyll from the eastern end of Legs 36 and 47 have been plotted. Despite the fact that the temperature profiles show that the top 15 m of the water column had been thoroughly mixed between Surveys 2 and 3, the depth and shape of the sub-surface chlorophyll maxima remained virtually the same.

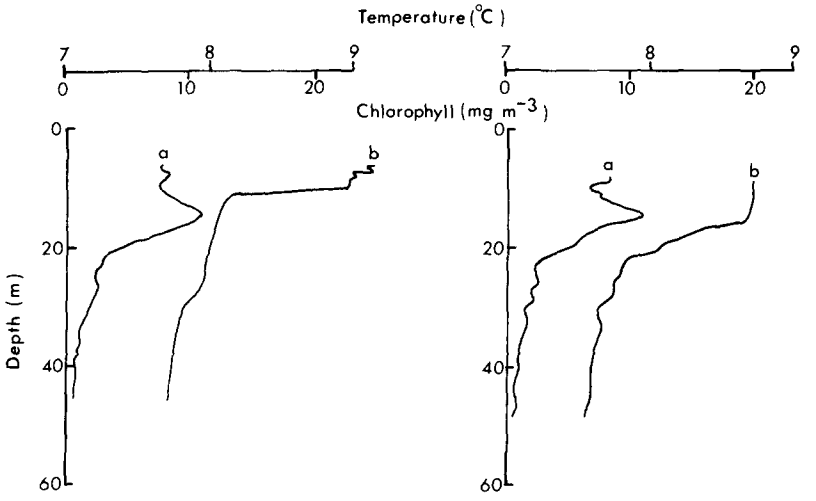

FIG. 17. Vertical profiles of (a) chlorophyll *a* (mg m^{-3}); (b) temperature (°C); at the eastern end of Leg 36 (Survey 2) and Leg 45 (Survey 3).

Another striking feature of these data was the vertical excursions of the chlorocline and thermocline suggesting strong internal wave activity. This is confirmed by contouring temperature and chlorophyll with σ_t as the vertical axis rather than pressure (Fig. 18), which removes most of the small-scale (2–6 km) horizontal variability.

4.3. *Changes in the surface abundance and distribution of phytoplankton species between Surveys 1 and 2*

Although the increase in levels of chlorophyll *a* was accompanied by an equivalent change in the total biomass of the phytoplankton as the water column became stratified, the species composition of the population was variable in both time and space (Table 1). On Survey 1 flagellates and three species of relatively large diatoms were the dominant taxa, with very few dinoflagellates. By Survey 2 all groups of phytoplankton were more abundant, but four species of small diatoms and a small unidentified dinoflagellate (*Gymnodinium* type) had increased most rapidly and together formed, on average, $>40\%$ of the total plant biomass, compared with $\sim 10\%$ on Survey 1.

A comparison of the distributions of individual species (Fig. 19) shows the differences more clearly. The large diatom species, as illustrated by data for *Lauderia borealis*, extended over the southern part of the survey area as the bloom developed, but their maximum cell densities in surface water increased only two- or three-fold. By contrast cell numbers for the small diatom species were generally 10–100 times greater on Survey 2, although their distributional patterns differed; on both surveys *Nitzschia delicatissima* and *Thalassiosira* sp A were widespread, whereas *Thalassiosira* sp B and *Skeletonema costatum* were largely confined to the somewhat colder, less saline water to the north. The occurrence of the unidentified dinoflagellate was patchy and showed no obvious relationship to hydrographic properties.

Levels of phaeopigments and protozooplankton carbon (mainly tintinnids and the non-photosynthetic dinoflagellates, *Protoperidinium* spp and *Dissodinium assymetricum*) suggest that there was a considerable grazing and, therefore, turnover of phytoplankton carbon even at the time of the first survey.

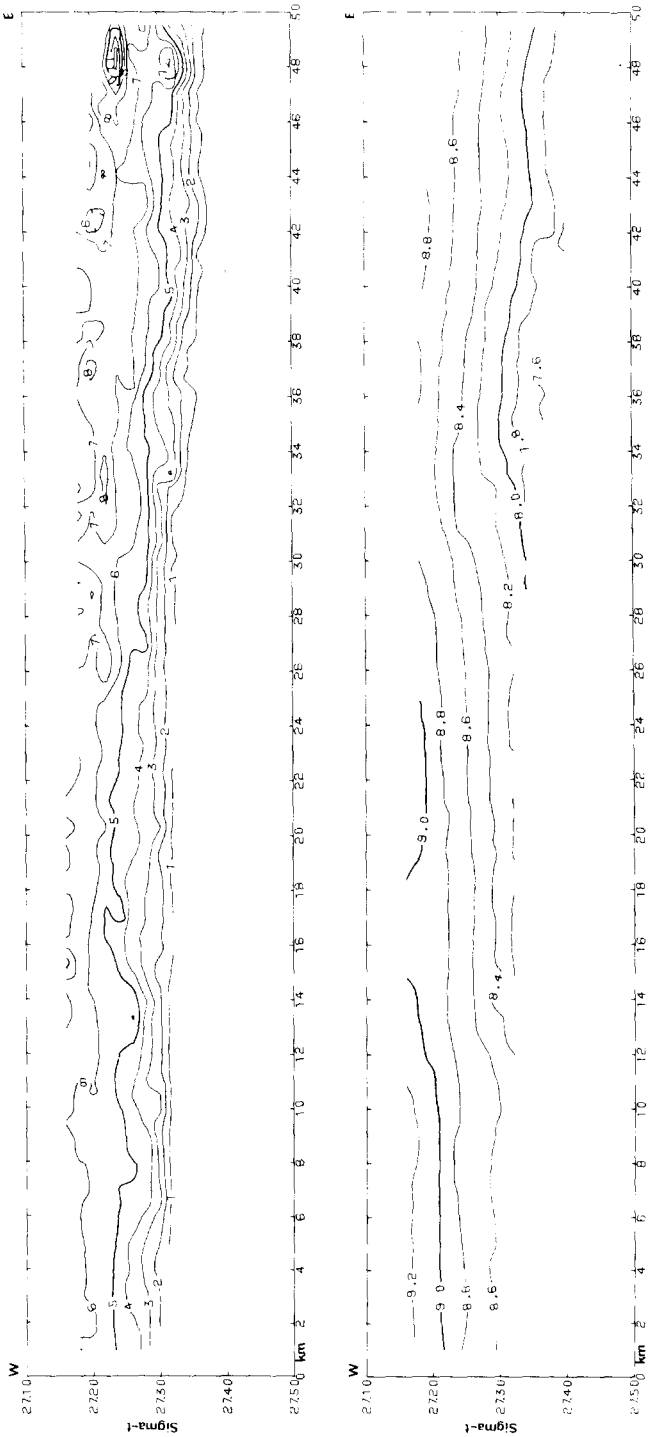

FIG. 18. Survey 3, Leg 47. Contoured sections of chlorophyll and temperature plotted against density (σ_t units $\times 10^2$).

TABLE 1. CHANGES IN THE PHYTOPLANKTON POPULATION BETWEEN SURVEYS 1 AND 2.
(Average values for 10 samples on Survey 1 and 9 samples on Survey 2, regularly spaced along alternate long legs of the Survey tracks)

	Survey 1	Survey 2	% Increase
Chlorophyll *a* ($\mu g\,\ell^{-1}$)	1.11	5.71	510
Phaeopigment ($\mu g\,\ell^{-1}$)	0.54	1.27	240
Total phytoplankton ($\mu g\,C\,\ell^{-1}$)	16.2	94.4	580
Protozooplankton ($\mu g\,C\,\ell^{-1}$)	6.4	21.7	340
Phytoplankton taxa[1] ($\mu g\,C\,\ell^{-1}$):			
Large diatoms[2]	4.1	17.6	440
Small diatoms[3]	1.4	27.2	1890
Other diatoms (41)	1.6	4.3	270
Unidentified dinoflagellate[4]	0.3	13.1	4360
Other dinoflagellates (18)	0.5	5.1	1020
Flagellates[5]	8.6	27.1	320

[1] Values in parentheses give number of species recorded.
[2] *Ditylum brightwellii, Lauderia borealis* and *Thalassiosira rotula*, with mean cell volumes of 27000, 21000 and 15000 μm^3 respectively.
[3] *Nitzschia delicatissima, Skeletonema costatum, Thalassiosira* sp. A and *Th.* sp. B, with mean cell volumes of 50, 190, 2650 and 150 μm^3 respectively.
[4] Small '*Gymnodinium*-type', with a mean cell volume of 270 μm^3.
[5] Unidentified naked forms, with a mean cell volume of 34 μm^3.

4.4. *Primary production measurements*

During the cruise four primary production experiments were made, one on Survey 1, two on Survey 2 and one on Survey 3. Only in the first experiment did the nitrate concentration exceed the minimum observed values of about 1 μM. The results are plotted in Fig. 20, with rate of carbon fixation normalised to chlorophyll biomass to give the units mg C [mg chlorophyll a]$^{-1}$ hr^{-1}. There was an increase in production up to irradiance values of between 30 and 70 W m^{-2}, and at higher light levels saturation followed by photo-inhibition of photosynthesis was observed. There is also evidence for a reduction in the assimilation number, P_m (rate of primary production per unit chlorophyll at optimal light intensity), between the first and last experiments which may have been related to the depletion of nitrate in the surface water or to changes in the species composition of the phytoplankton (see footnotes to Table 1). Another interesting feature of the experiments was the observed variations in levels of chlorophyll *a* during the incubation period. With the population dominated by flagellates (experiment 1); chlorophyll increased by as much as 0.10 hr^{-1} in the light and dark bottles. The reverse occurred in the other experiments, with decrease as great as 0.05–0.10 hr^{-1} for diatoms exhibiting photo-inhibition of carbon fixation under high light intensities (experiments 3 and 4) and 0.03 hr^{-1} for the dinoflagellate population in the dark bottle (experiment 2).

Since only a few measurements of primary production were made of each population type, a single photosynthesis light curve, based on the equation of PLATT, GALLEGOS and HARRISON (1980) has been fitted to all the data. This is discussed in further detail in Section 5.5.

4.5. *Carbon to chlorophyll and carbon to nitrogen ratios*

Data on the relationships between particulate organic carbon (POC) and nitrogen (PON), phytoplankton carbon (PC), and chlorophyll *a* are summarised in Fig. 21. Regression lines were

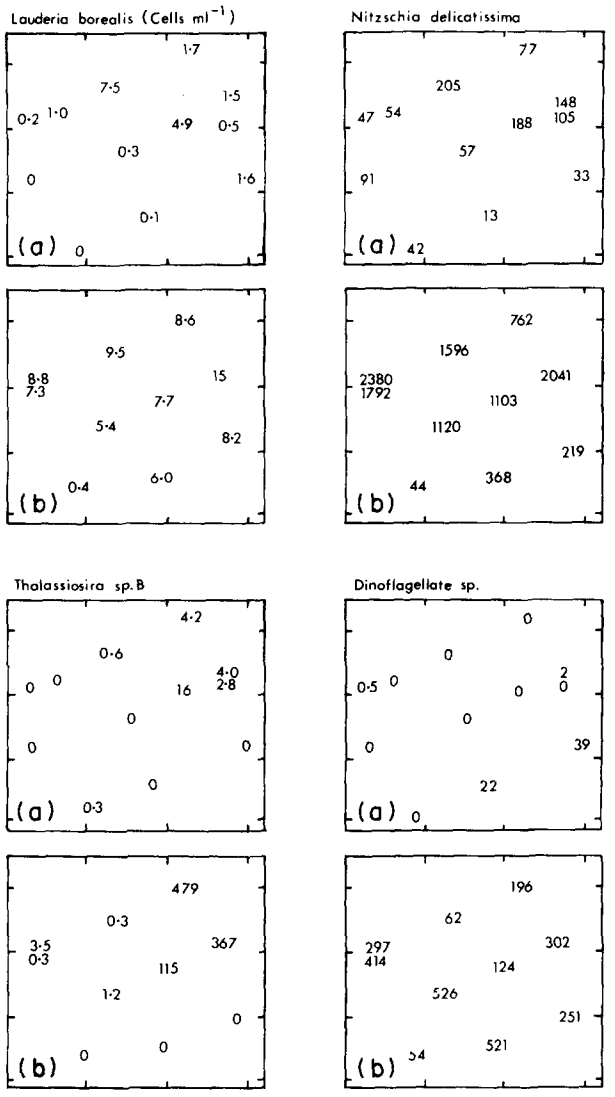

FIG. 19. Surface concentration (cells mℓ^{-1}) of four phytoplankton species on Surveys 1 (a) and 2 (b).

obtained by the reduced major axis method (YORKE, 1966) which allows for sources of error in both variables. Measurements made in the Celtic Sea in the following year (14–30 April, 1980) have been included in the figures to show that the conclusions drawn from the 1979 data are generally valid for this region. Since all the observations are restricted to a 2–3 week period corresponding to the development of the spring phytoplankton outburst, problems of interpretation due to temporal changes in the relative proportion of different components of particulate material (see BANSE, 1977) should be minimal.

The regression line for POC against chlorophyll gives a particulate carbon-to-chlorophyll ratio of 63 [Fig. 21(a)] for the 1979 data. For a given type of phytoplankton population growing under relatively uniform hydrographic conditions (in this case, spring diatoms in a weakly

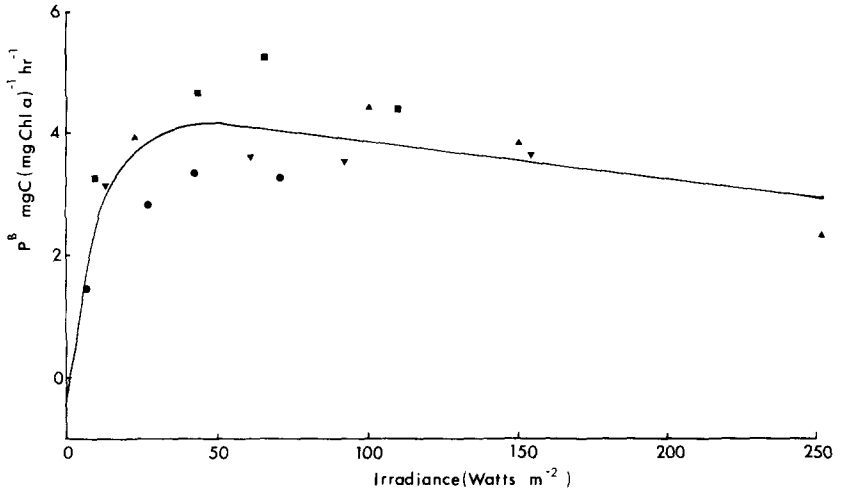

FIG. 20. Relationship between surface irradiance (watts m^{-2}) and rates of photosynthetic carbon fixation (mg C [mg chlorophyll a]$^{-1}$ hr^{-1}) measured in a deck incubator during Surveys 1 (■); 2 (●, ▲) and 3 (▼). The dominant phytoplankton taxa in each experiment were flagellates (■), small diatoms (●, ▼) and dinoflagellate sp B (▲) – see notes to Table 1.

stratified water column with inorganic nutrients available or only recently depleted), it is reasonable to assume that changes in PC, derived from cell counts, and chlorophyll *a* will be linearly related [Fig. 21(c)]. The slope of this regression gives a phytoplankton carbon-to-chlorophyll ratio of 17. The scatter about the regression line between these two parameters is to be expected in view of the inherent errors in estimating PC and also because of diel variations in carbon and chlorophyll per cell (see HUNTER and LAWS, 1981). Both the magnitude and wide variation of POC values for any given chlorophyll or PC concentration [Figs 21(a, b)] suggest, therefore, that a substantial amount of POC (50–100 $\mu g\ C\ \ell^{-1}$ as shown by the intercepts on the POC axes) was not associated with the phytoplankton at the start of the bloom and that large quantities of non-phytoplankton POC were generated, presumably by secondary production processes, as the plant biomass increased. These effects are clearly illustrated by the attempt to fit [Fig. 21(b)] the empirical relationship between PC and POC derived by EPPLEY, HARRISON, CHISHOLM and STEWART (1977). If the initial non-phytoplankton component is first subtracted from the observed POC values, there is some agreement between predicted and estimated values of PC at low POC levels but not at high POC levels. The equation of EPPLEY, HARRISON, CHISHOLM and STEWART (1977) gives a mean phytoplankton carbon to chlorophyll ratio of 45 for the April 1979 POC data.

In order to determine the growth rate of phytoplankton from rates of carbon fixation an accurate value for the carbon-to-chlorophyll ratio is required. EPPLEY, HARRISON, CHISHOLM and STEWART (1977) regarded the direct cell count method of determining PC the best one currently available. Since cell volumes of the dominant species varied by nearly three orders of magnitude (see footnotes to Table 1) and a linear relationship between PC and chlorophyll was found [Fig. 21(c)], it appears that the general equation for converting cell volume to cell carbon is appropriate. The observed PC to chlorophyll ratio of 17 is similar to values obtained by EPPLEY, HARRISON, CHISHOLM and STEWART (1977) using the same method (see their Fig. 5a) for diatom populations in coastal waters off California. However, the best independent check on this ratio from field data is provided by observations on spring

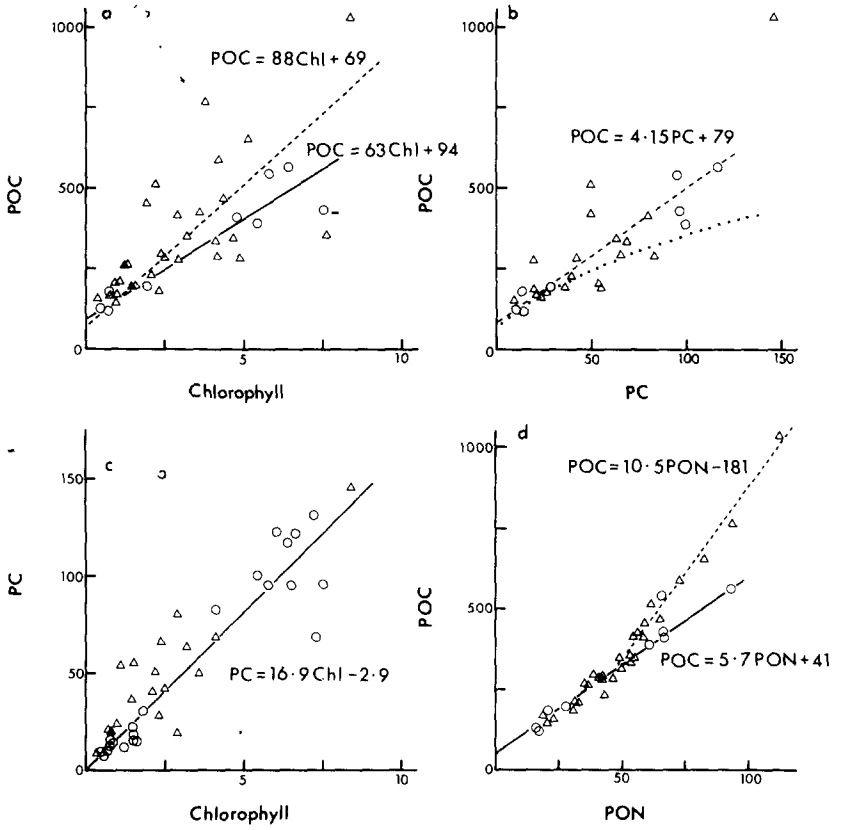

FIG. 21. Relationships between particulate organic carbon (POC) and nitrogen (PON), phytoplankton carbon (PC), and chlorophyll *a* for samples collected in 1979 (○) and 1980 (△). Regression lines are drawn for 1979 data alone (solid lines) and for 1979 + 1980 data combined (dashed lines). The upper right hand point in (b) was ignored for the regression analysis. All units are given in mg m^{-3}. The dotted curve in (b) is derived from the empirical relationship PC = 0.158 (POC) + 0.007 (POC)^2 given by EPPLEY, HARRISON, CHISHOLM and STEWART (1977). The dashed curve in (d) is based on the high POC (> 400 mg C m^{-3}) samples obtained in 1980.

diatom populations under conditions of little or no grazing, when POC is composed mainly of PC and can be directly related to chlorophyll. Thus, TETT, COTTRELL, TREW and WOOD (1975) found a POC to chlorophyll ratio of 17 for Loch Creran in mid-March and STEELE and BAIRD (1962) a ratio of 23 for the central North Sea in April. These values must be considered as upper limits for the phytoplankton carbon to chlorophyll ratio since some non-phytoplankton POC is likely to have been present. On this basis, our estimates of PC appear to be realistic and indicate [Fig. 21(b)] that, during the spring phytoplankton outburst in the Celtic Sea, PC forms only 10–20% of total POC, the higher proportions occurring as the phytoplankton biomass reaches a maximum. Data for Surveys 1 and 2 suggest that, as the average PC increased from 16 to 94 μg ℓ^{-1} (Table 1), as much as 400 μg C ℓ^{-1} of non-phytoplankton carbon was produced in the surface water.

Another independent check on the carbon-to-chlorophyll estimates can be made by combining them with the ^{14}C results to calculate daily growth rates and then comparing these values with the growth rate estimates of EPPLEY (1972), which were obtained from cell counts in

culture experiments. If an assimilation number of 4 mg C [mg chlorophyll a]$^{-1}$ hr^{-1} is assumed (Fig. 20) and if growth is assumed to last 12 hr then the growth rate in doublings per day will be 4.0, 1.5 and 1.0 for carbon-to-chlorophyll ratios of 17, 45 and 63 respectively. According to EPPLEY (1972) the maximum expected growth rate at 10°C would be 1.6 doublings per day. It is clear that the growth rate for carbon-to-chlorophyll ratios of 45 and 63 falls below this maximum whereas that for 17 is considerably larger. This presents a dilemma in that the supposedly most accurate method of determining PC yields a phytoplankton growth rate that is three times that observed in culture experiments. It is of course possible that the estimates of PC are correct but that the error lies in the estimates of either chlorophyll concentration or ^{14}C assimilation. However this dilemma cannot be resolved with our present data and it can only be concluded that the carbon-to-chlorophyll ratio lies somewhere in the range 17 to 63. This problem will be returned to later in the paper.

The plot of POC against PON [Fig. 21(d)] gives a carbon to nitrogen ratio of 5.7, identical with the 'Redfield ratio'. The 1980 samples fall very close to this line, except for high POC ($> 400\,\mu$g C ℓ^{-1}) samples which showed a C:N ratio of 10.5. The latter were mainly collected from water with a low ($< 0.2\,\mu$M) nitrate content, and may reflect nitrogen limitation of phytoplankton growth. A similar increase in particulate carbon to phosphorus ratios was observed by TETT, COTTRELL, TREW and WOOD (1975) in Loch Creran as the phytoplankton biomass started to decline.

5. QUANTITATIVE ANALYSIS OF THE PHYSICAL AND BIOLOGICAL CHANGES

5.1. *The role of advection*

In the previous section the changes in the physical and biological variables between the three surveys were described in a qualitative manner. Before attempting to quantify these changes by relating averaged vertical profiles from the three surveys some means must be found of removing the effects of horizontal advection. The currents in the area will consist of a predominant tidal component and a residual. The effect of tidal motion has already been allowed for in calculating track positions and so in this section the possible effect of the residual currents are considered. No direct observations on currents were obtained on the cruise and so information has been derived from a theoretical model and the σ_t sections.

PINGREE and GRIFFITHS (1980) have developed a vertically integrated numerical model of the wind-driven currents on the continental shelf. A steady wind stress was imposed on a model of the M_2 tide and the resultant currents were averaged over a tidal cycle to yield residual currents. The results were presented for 20 knot south-easterly and south-westerly winds, being typical of summer and winter conditions respectively. For a south-westerly wind the model predicted a strong current (~ 10 cm sec^{-1}) around the SW corner of Ireland which continued eastwards along the southern coast. Between 7° and 6°W part of this current turned southwards across the Celtic Sea with velocities ranging from 1 to 3 cm sec^{-1}. It will be remembered that the σ_t sections obtained by the undulator implied a south to south-east trending geostrophic current and it is tempting to identify this current with the current of the Pingree–Griffith's model.

In Fig. 22 the geopotential anomaly between 15 m and 50 m has been plotted for Legs 9, 34 and 45. A steep change in this anomaly took place in the HGZ on all three surveys, although the noise level was higher on Leg 45, probably caused by the deeper thermocline. These results show that the σ_t gradient was not transitory, and an order of magnitude calculation gives a

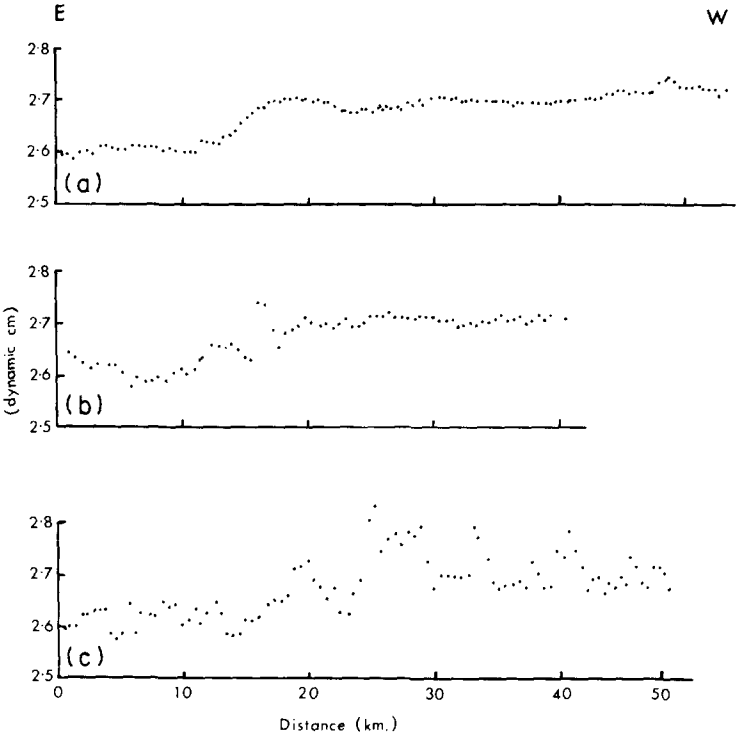

FIG. 22. Geopotential anomaly (dynamic cm) from east to west between 15 and 20 m for (a) Leg 9 on Survey 1; (b) Leg 34 on Survey 2; and (c) Leg 45 on Survey 3.

geostrophic current in the HGZ of 1 cm sec^{-1}. There are of course a number of problems in using the geostrophic method in shallow water (COOPER, 1960), such as the absence of a level of no motion and the unlikelihood of an equilibrium developing if winds are changing daily. However, the fact that the direction and strength of the geostrophic current agrees with the Pingree–Griffiths model lends support to this interpretation, although it should be stressed that this model is not strictly applicable to a stratified water column.

It is also interesting to compare these results with those of COOPER (1961), who carried out a hydrographic survey of this area in April 1950. Cooper postulated a number of currents based mainly on a study of semi-conservative properties and the theoretical wind drift for the prevailing south-westerly winds (COOPER, 1960). These currents show a large measure of qualitative agreement with the Pingree–Griffiths model, especially the current trending southwards across the Celtic Sea which Cooper called the Nymphe Bank Current. He presented an east–west section along 51°20′N which passes through our survey area and it is interesting to note that his Nymphe Bank current separates zones of high and low horizontal temperature and salinity gradients, as is the case with the postulated current on our survey.

We have seen that a number of strands of evidence all point to a residual current in the area which could be as high as 3 cm sec^{-1} in the HGZ, but will probably be much less than this elsewhere. If a conservative value of 1 cm sec^{-1} is assumed then, in the eight days between Surveys 1 and 3 a parcel of water would have drifted 7 km. A drift of this order will not drastically change the overall spatial pattern of the variables, as is supported by the similarity of the salinity data for all three surveys. However, it will be significant when attempting to compare

quantitatively vertical profiles of temperature or chlorophyll from the three surveys especially in the SW where the horizontal gradients were large. Furthermore, it has been suggested that in between Surveys 2 and 3 wind-induced surface drifts of up to 5 cm sec^{-1} may have occurred. A method of dealing with this problem will be presented in the next section.

5.2. *Heat budget method of determining equivalent profiles*

In the next section we will attempt to estimate vertical profiles of eddy diffusion and net phytoplankton growth rate using what will be termed equivalent profiles from the three surveys. By the term equivalent profiles we mean profiles from the same body of water in a Lagrangian sense. In practice this is almost impossible to achieve and it has already been seen that even a small residual current of 1 cm sec^{-1} could have a significant effect. An indirect method of selecting equivalent profiles has therefore been used based on the calculated heat input to the water column.

The method involves the following stages:

(i) Two positions, A and B, were selected at either end of Leg 9 (see Fig. 23) as typical of the different conditions in the east and west of the survey area.

(ii) Using the undulator data a horizontal profile of the depth averaged temperature between the surface and the bottom (taken as 100 m) was calculated for Legs 9 and 34 (Fig. 23). The undulator did not sample the total water column and so in order to calculate this quantity it had to be assumed that the undulator had penetrated the bottom mixed layer. This assumption would appear to be justified in most cases.

(iii) Using the meteorological data the heat input to the water column between Surveys 1 and 2 was calculated (see Appendix A for details). It was then a simple matter to calculate the expected increase in average temperature between these two surveys.

(iv) This calculated increase was then added on to the mean temperature profile for Leg 9, which was overlayed on the mean temperature profile for Leg 34. One profile was then moved horizontally until a good match between profiles was obtained for either position A or B.

This procedure gives the position on Leg 34 with a mean temperature that would be predicted from the known heat input. It can then be assumed that no advection has taken place between the two positions between Surveys 1 and 2 otherwise this woud have reduced or increased the mean temperature. Equivalent profiles on Legs 9 and 34 have now been identified and a similar procedure can be used for Leg 45. The positions of A and B obtained for the three surveys are marked on Figs 6, 9 and 14.

There are three main sources of error in this technique. The first arises from the assumption that the temperature distribution below the bottom of the undulator cycle was isothermal. The contoured sections show that this assumption was likely to be more accurate at position B than position A. However as the horizontal gradients of temperature and chlorophyll at A are weak this should not contribute any substantial error when eddy diffusivities and phytoplankton growth rates are calculated. Secondly, a geostrophic current, which will not transport heat, being broadly parallel with the isotherms, may well transport phytoplankton thus producing errors in the calculated phytoplankton growth rates. However the two chosen positions were some distance either side of the HGZ and so errors arising from this source will be minimal.

Finally errors will be introduced by wind-induced drift causing relative movement of water above and below the thermocline. This source of error will be most severe at position B where there was a substantial horizontal gradient of temperature below the thermocline. In Section 4.2.3 it was suggested that the wind induced shear may be as much as 5 cm sec^{-1} between

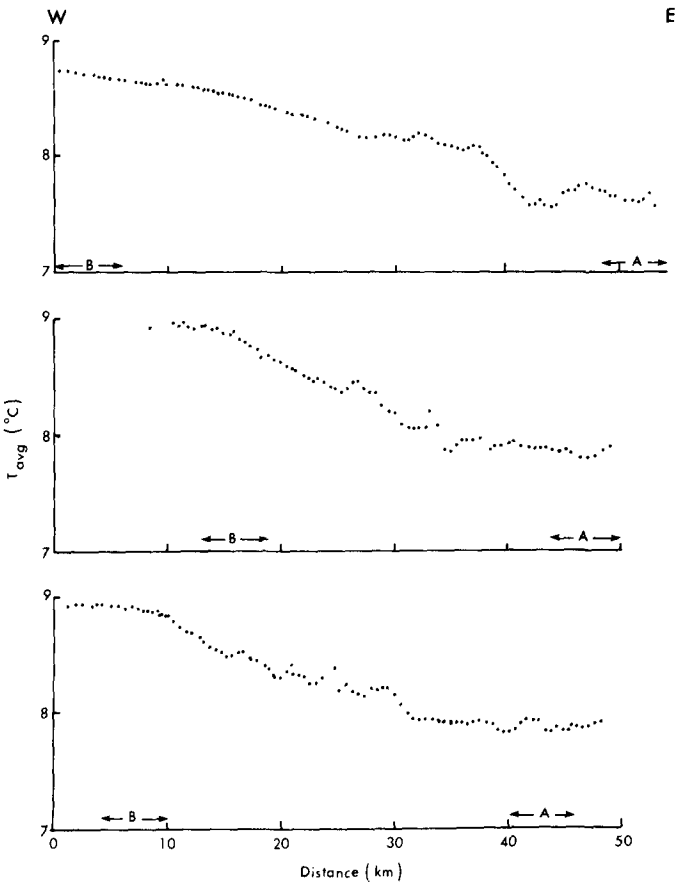

FIG. 23. Mean temperature (°C) between surface and 100 m for (a) Leg 9 on Survey 1; (b) Leg 34 on Survey 2; (c) Leg 45 on Survey 3. The horizontal averaging scales for positions A and B are shown for each leg.

Surveys 2 and 3. Therefore in two days the surface water might move up to 8 km relative to the bottom water. This would be equivalent to a 0.4°C change in the temperature of the bottom water (see Fig. 15). The changes in average temperature of the water column due to this advective shear are therefore greater than that due to surface heating (see Appendix A, Table 3) and so for position B between Surveys 2 and 3 the results must be treated with caution. However for position A, where the horizontal gradients are virtually zero, and for position B between Surveys 1 and 2 when wind speeds were much less, the profiles produced by this method should give a more accurate representation of the changes between surveys than by simply using geographical position.

The problem of removing the effect of internal waves will now be considered. The coherence between the depth of the chlorocline and pycnocline has already been noted. On Leg 45 for instance there were vertical excursions of the chlorocline of up to 20 m with wavelengths of from 4 to 8 km. If meaningful comparisons of vertical profiles between surveys are to be made these effects must first be removed by some method of spatial averaging. The horizontal averaging distance must be larger than the mean wavelength of the internal waves but not so large as to obscure the horizontal differences that we wish to investigate. Accordingly a distance of

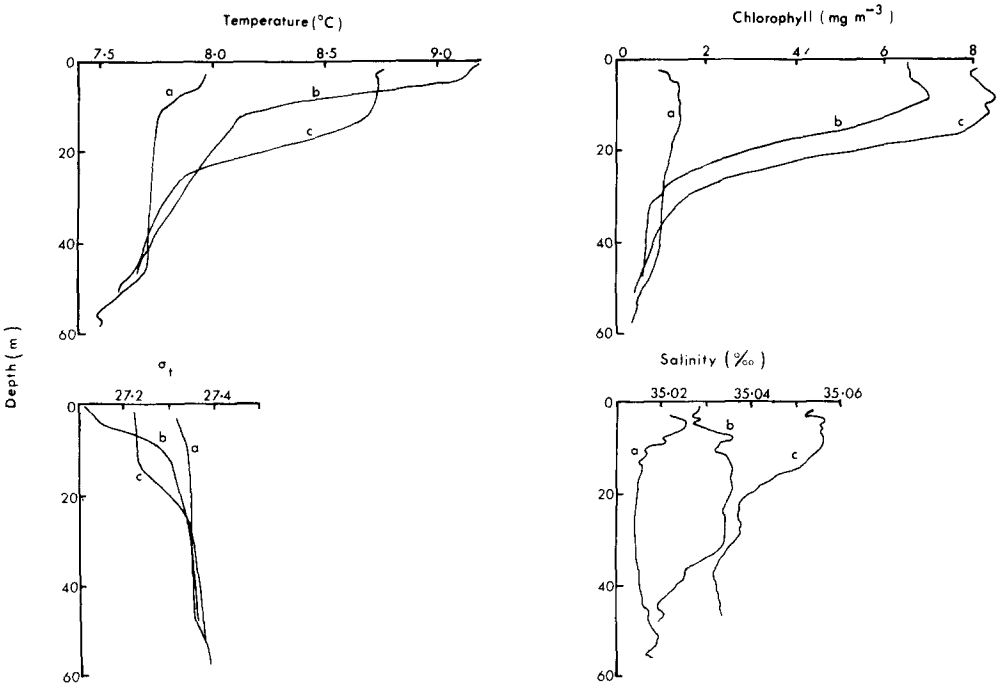

FIG. 24. Average vertical profiles at positions A of temperature (°C), chlorophyll *a* (mg m^{-3}), density (σ_t units) and salinity (‰) for (a) Survey 1; (b) Survey 2; (c) Survey 3. Details of data averaging techniques to obtain these profiles are given in the text.

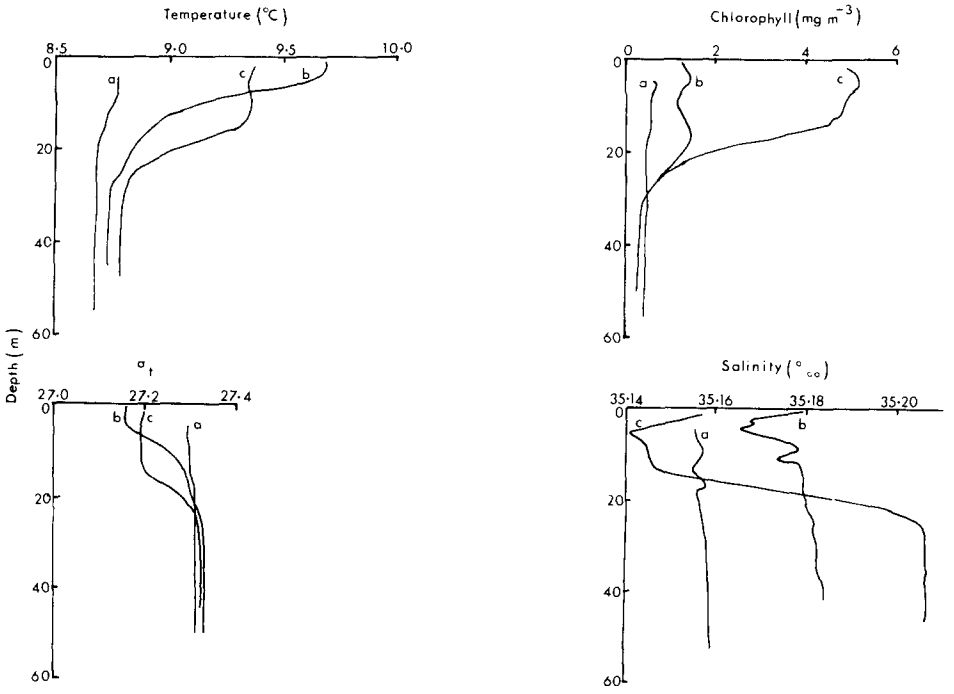

FIG. 25. Average vertical profiles at position B of temperature (°C), chlorophyll *a* (mg m^{-3}), density (σ_t units) and salinity (‰) for (a) Survey 1; (b) Survey 2; (c) Survey 3.

6 km was chosen and the averaging process was carried out as follows. Firstly, for each undulator profile, within a distance of 3 km either side of the required position, (see Fig. 23) the half-second values of a given variable were averaged over successive 1 m depth intervals. These smoothed depth profiles were then themselves averaged to give a final mean profile for each variable. The results of this process for temperature, salinity, chlorophyll and σ_t for positions A and B are plotted in Fig. 24 and 25. These profiles will be analysed in the next few sections.

5.3. *The temporal change in the physical variables at positions A and B*

The temperature profiles emphasise the main changes referred to in earlier sections. At position A on Survey 1 there was a shallow and a deep thermocline with a layer of virtually isothermal water between the two. In between Surveys 1 and 2 the surface heating caused a considerable development of the shallow thermocline, while the deep thermocline was eroded away. In between Surveys 2 and 3 the increased wind mixing produced a deepening of the surface mixed layer. The same sequence of events was evident at position B although there was no evidence there of the deep thermocline, and the top-to-bottom temperature difference was always less than that for A. The profiles for σ_t show that this quantity is controlled mainly by temperature.

The sequence of events in the thermal structure reported here are typical for this period of the year when stratification is beginning to be established (JAMES, 1980). The east–west differences in the degree of stratification found on this survey were also noted by PINGREE, HOLLIGAN, MARDELL and HEAD (1976) in April 1975 and they attributed these differences to differences in tidal mixing. The effects of tides on stratification in shelf areas has been thoroughly investigated in recent years (SIMPSON, HUGHES and MORRIS, 1977: PINGREE and GRIFFITHS, 1978) and can best be parameterised by the quantity $S = \log_{10}(h/c_d\langle|u|^3\rangle)$, where h is water depth, c_d the bottom drag coefficient and u the tidal stream velocity. It has been found empirically that an S-value of 1.5 marks the boundary between water that would be well-mixed in summer from that which would be stratified. In Fig. 26 we have plotted contours of S derived from the numerical model of PINGREE and GRIFFITHS (1978). The values range from 2.5 to 3 which are typical of stratified water as would be expected. However, within the survey area S is highest in the NE and lowest in the SW. This would imply that, for a given value of heat input and wind speed, stratification would develop first in the NE and gradually spread to the SW which is in agreement with our observations.

There is also another factor that would favour the development of stratifications in the NE. The sensible heat flux is proportional to the quantity $T - T_s$ where T is the air temperature and T_s the sea temperature (see Appendix A). This means that the lower the sea temperature the greater will be the sensible heat flux from the atmosphere to the water. The sea temperature was always lower in the NE compared to the SW and so, other factors being equal, the water in the NE will heat up faster.

Thus we have two effects which would favour the development of stratification in the NE. Whether these two factors are enough to account quantitatively for the observed differences between positions A and B can only be decided by using a model such as that of JAMES (1977). Such an approach is beyond the scope of the present paper and we will instead use the equivalent temperature profiles to calculate eddy diffusion coefficients K_z.

The method used for this follows closely that described by JASSBY and POWELL (1975). The equation governing the temperature $T(z, t)$ at depth z and time t is

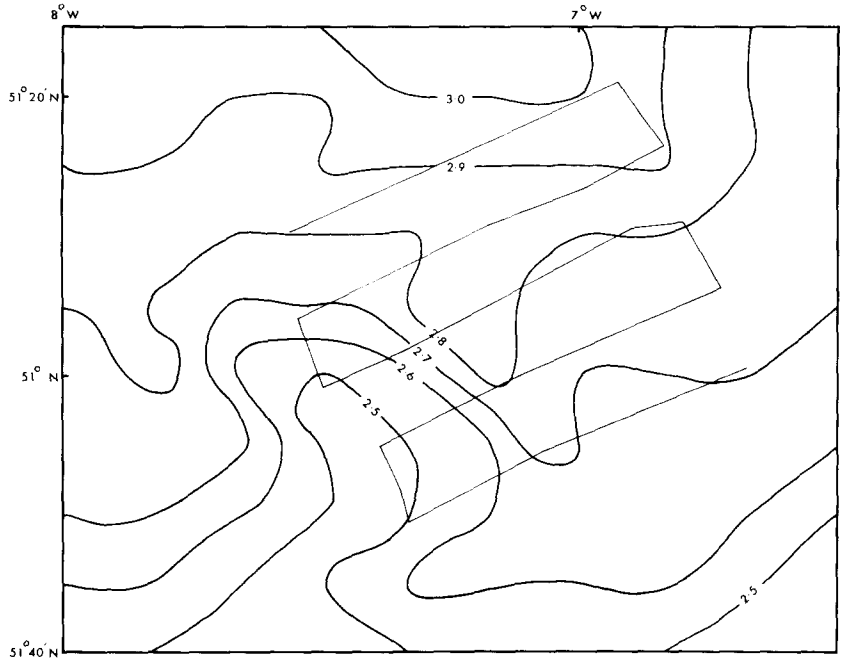

FIG. 26. Contours of the stratification parameter, S, given by the numerical model of PINGREE and GRIFFITHS (1978) for the survey area.

$$c\rho \frac{\partial T}{\partial t} = c\rho \frac{\partial}{\partial z}\left(K_z \frac{\partial T}{\partial z}\right) - \frac{\partial R_z}{\partial z} \tag{1}$$

where c is the specific heat of sea water, ρ its density and $R_z = R(z, t)$ is the flux of solar radiation. If equation (1) is integrated from a depth z down to a depth z_m, the average depth of the bottom of the undulator cycles, we obtain

$$\frac{\mathrm{d}}{\mathrm{d}t}\int_z^{z_m} T(u, t)\mathrm{d}u = -K_z \frac{\partial T}{\partial z} - F + R_z/\rho c \tag{2}$$

where F is the downward heat flux from depth z_m. The L.H.S. of equation (2) and $\partial T/\partial z$ can be estimated from the change of equivalent temperature profiles between two surveys, while the quantities F and R_z can be estimated from the meteorological data and the estimated solar radiation absorption properties of the water (Appendix B). It is thus possible to use equation (2) to calculate values of K_z from just below the surface to the depth z_m. These values will be average values for the period between two surveys and will ignore the fact that K_z will actually be changing with time (JAMES, 1977). The profiles of K_z observed by this method for the two time period (Surveys 1–2 and 2–3) for positions A and B are plotted in Figs 27(a) and (b).

For the first time period the eddy diffusivity at both positions showed a minimum of 1–2 $cm^2 sec^{-1}$ at a depth between 5 and 10 m. Above and below this minimum, which is coincident with the thermocline, the eddy diffusion increased by an order of magnitude. For the period between Surveys 2 and 3 the eddy diffusivity minimum moved below 20 m reflecting the downward movement of the thermocline.

Once a stable thermocline has been established then the turbulent diffusion above and below

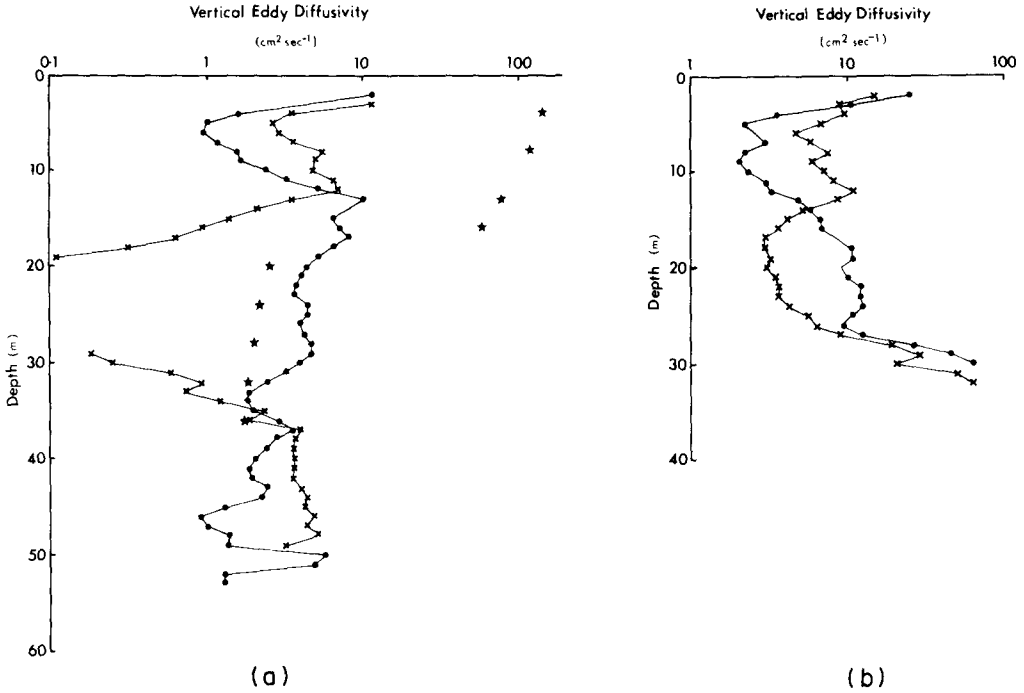

FIG. 27(a). Profiles of vertical eddy diffusivity ($cm^2 sec^{-1}$) at position A for the period between Surveys 1 and 2 (•—•) and between Surveys 2 and 3 (X—X). Details of the method of calculation are given in the text. Values marked with an asterisk were obtained from the numerical model of JAMES (1977).

FIG. 27(b). Profiles of vertical eddy diffusivity ($cm^2 sec^{-1}$) at position B for the periods between Surveys 1 and 2 (•—•) and between Surveys 2 and 3 (X—X).

it will be controlled by wind and tidal mixing respectively, with the two layers being effectively shielded from the other by the thermocline (JAMES, 1977). It is thus interesting to note that for both time periods the eddy diffusivity below the thermocline was an order of magnitude higher at position B compared to position A, whereas above the thermocline the values were comparable. This is consistent with the suggestion made earlier that the differences in stratification at A and B were due mainly to differences in tidal mixing.

In Fig. 27(a) we have also plotted the eddy diffusivities predicted by James's model of the seasonal development of the thermocline (JAMES, 1977). This model predicted the annual cycle of temperature and eddy diffusivity given the annual cycles of solar radiation, dew point, wind speed and tidal current at four positions in the Celtic Sea. These ranged from a well-mixed position to the north of the St David's Head front (SIMPSON, HUGHES and MORRIS, 1977) to a stratified position that was within the area of the present survey. The starting condition for the model was a completely mixed temperature profile in mid-March and the model predicted that by mid-April the top-to-bottom temperature difference was 0.06°C increasing to 2°C by mid-May. This is a much slower development of the thermocline than observed in mid-April 1979 which was closer to the mid-May of the model. Accordingly it is the mid-May eddy diffusivities that have been plotted in Fig. 27(a). It can be seen that the variation of eddy diffusivity with depth agrees qualitatively with eddy diffusivities calculated between Surveys 2 and 3. Quantitatively the theoretical values are generally an order of magnitude higher. James's model

used monthly averages of the meteorological data obtained over 14 years and so the differences between the results, at least above the thermocline, might by explained by the better than average weather conditions experienced in April, 1979 combined with neap tides over the survey period.

The salinity profiles showed that there were changes in the estimated mean salinity at positions A and B between surveys, especially at position B. This may reflect the fact that the horizontal contours of salinity and temperature are not parallel so that any advection would have a different effect on the two variables at a given position. The development of the haloclines has already been discussed.

5.4. *Temporal change in chlorophyll at positions A and B*

Some time has been spent analysing the hydrographic changes that took place in order to provide a firm physical background for the analysis of the changes in the vertical distribution of chlorophyll. The chlorophyll profiles for position A and B (Figs 24, 25) show that there were significant differences in the way that the bloom developed at the two positions. At A the main growth in the surface layers took place between Survey 1 and 2 with the growth slowing down between Survey 2 and 3, whereas at B this situation was reversed. It is possible that the increase in chlorophyll at B between Survey 2 and 3 may have been overestimated. The position of B on Survey 2 was just to the SW of an area of steep horizontal chlorophyll gradient and so if the heat budget method failed to adjust sufficiently for the south-westerly surface drift which occurred over this period then part of the observed increase may be advective in origin. As discussed earlier on Survey 2 the chlorocline was around 10 m deeper than the thermocline but by Survey 3 they were at the same depth.

If the chlorophyll concentration at depth z and time t is given by $C(z, t)$ then using the chlorophyll profiles a net growth rate g for chlorophyll between two surveys can be calculated from

$$g(z) = \ln (C(z, t_2)/C(z, t_1))/\Delta t \tag{3}$$

where Δt is the time difference between the two surveys. By the term net growth rate we mean the phytoplankton growth remaining after other losses from grazing, diffusion or sinking have taken place.

Plots of g at A and B for the time periods between Surveys 1 and 2 and Surveys 2 and 3 are given in Fig. 28. For the first time period at position A the net growth rate above 15 m was between 0.2 and 0.3 day^{-1}. Below 15 m the net growth rate dropped sharply to reach zero at 28 m. At position B for the same period the growth rate above 15 m was about a third of that at A. Unlike the curve for A there was a peak in the growth rate at 17 m but the depth of zero net growth was 29 m, very similar to that at A. It should be noted that the latter depth was deeper than the 1% light level which at the end of Survey 2 was between 15 and 17 m. For the second time period the growth rate at B above 15 m had increased to 0.5–0.7 day^{-1} and the depth of zero net growth had decreased to 24 m. These results support the suggestion made in Section 5.2.3 that the population in the west of the survey area was initially growing at a slower rate than that in the east but later grew faster.

The curve of growth rate at A for the second time period is very different from the other three curves. Above 15 m the net growth rate was ~ 0.1 day^{-1} confirming that in the east the surface population growth was slowing down by the third survey. However, below 15 m the net growth rate increased to ~ 0.3 day^{-1}, remained at this level down to 35 m, thereafter declining without ever becoming negative. It is interesting to note that the high growth rates occurred in

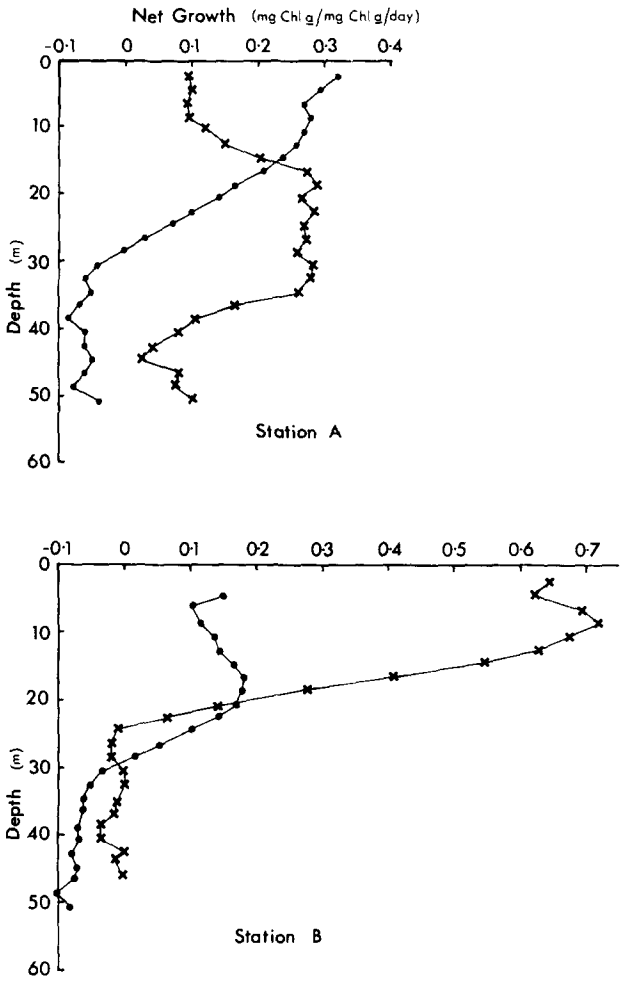

FIG. 28. The net growth in the standing stock of chlorophyll (mg chlorophyll *a*/mg chlorophyll *a*/day) for the periods between Surveys 1 and 2 (•—•) and between Surveys 2 and 3 (X—X) at positions A and B.

and just below the thermocline where the eddy diffusivity is very low (Fig. 27). This suggests that at A the bloom had reached the stage at which growth in the surface layers was declining, due to either nutrient limitation, grazing pressure or a combination of both, and that the main growth was now taking place at the base of the thermocline where the nutrient levels were still high (Fig. 13). This would be consistent with the observed development of sub-surface chlorophyll maxima in the NE of the survey area (see Sections 4.2.2 and 4.2.3) where presumably the bloom was even more advanced than at A.

The results of this and previous sections can be summarised into four main observations about the phytoplankton growth during the three surveys.

(i) Between Surveys 1 and 2 the net growth rate in the top 20 m was higher at A than at B. Between Surveys 2 and 3 the position was reversed and the net growth at B was higher than that observed at A for either period, although the possibility that part of the growth at B may have been advective in origin cannot be excluded.

(ii) Between Surveys 2 and 3 the net growth at A was low in the top 10 m and rose to a broad maximum in the thermocline.

(iii) At the beginning of Survey 2 the top of the chlorocline was 10 m deeper than the top of the thermocline.

(iv) The sub-surface chlorophyll maxima observed in the NE of the survey area on Surveys 2 and 3 were apparently unaffected by the increased vertical mixing caused by the increase in wind speed.

5.5. *A quantitative model of phytoplankton growth*

The net change in phytoplankton at a given depth over a period of time is the sum of a number of processes of which primary production, sinking, diffusion, nutrient limitation and grazing are probably the most important. All of these processes are likely to vary with time and depth, and some understanding of how they combine to produce the observed net growth of phytoplankton is only possible using a mathematical model. A number of such models of varying degrees of complication have been developed in recent years (WINTER, BANSE and ANDERSON, 1975; JAMART, WINTER, BANSE, ANDERSON and LAM, 1977; WROBLEWSKI, 1977; RADACH, 1980; HORWOOD, 1982) and the model used here draws on these results. However, our model is comparatively simple and is based on those processes for which we have good measurements and ignores those processes or quantities for which the field data are inadequate. It is intended to be an explorative model in a first attempt to understand quantitatively the observations described above.

The modelled variables are phytoplankton chlorophyll concentration $C(z, t)$ measured in mg chlorophyll a m^{-3} and nitrate–nitrogen concentration $N(z, t)$ measured in μM. Both quantities can vary with depth z and time t and the equations describing their net change with time at a given depth are

$$\frac{\partial C}{\partial t} = rC - b - \frac{\partial}{\partial z}(vC) + \frac{\partial}{\partial z}\left(K_z \frac{\partial C}{\partial z}\right) \tag{4}$$

$$\frac{\partial N}{\partial t} = -q + \frac{\partial}{\partial z}\left(K_z \frac{\partial N}{\partial z}\right)$$

where $r = r(I, N)$ is the net primary production, $b = b(C)$ the grazing rate, v the phytoplankton sinking velocity, K_z the eddy diffusivity, $q = q(C)$ the nutrient uptake rate and $I = I(z, t)$ is the irradiance in the photosynthetic range (350–700 nm). As the model only considers nitrate-nitrogen no allowance is made for regeneration of nutrients by zooplankton excretion. Each of these parameters will now be studied in more detail.

5.5.1. *The primary production–irradiance relationship.* Primary production is generally considered to be a function of light irradiance and nutrient concentration, and a number of different equations have been suggested to model this relationship (PLATT, DENMAN and JASSBY, 1977). To model the relation with light we will use the equation recently suggested by PLATT, GALLEGOS and HARRISON (1980) which allows for photo-inhibition. The gross primary production $P_g(I)$ is given by:

$$P_g(I) = P_s\left[1 - \exp\left(\frac{-\alpha I}{P_s}\right)\right] \exp\left(\frac{-\beta I}{P_s}\right), \tag{5}$$

where P_g is the gross production normalised to chlorophyll biomass (units mg C [mg chlorophyll a]$^{-1}$ hr^{-1}), I is the irradiance, and α, β, P_s are parameters of the curve to be estimated from the data. The term α represents the slope of the production–light curve at the origin and β is the parameter that represents photo-inhibition. The parameter P_s is related to the assimilation rate P_m (the gross production at optimal light intensity) by the relation:

$$P_m = P_s\left(\frac{\alpha}{\alpha+\beta}\right)\left(\frac{\beta}{\alpha+\beta}\right)^{\beta/\alpha} \tag{6}$$

Equation 5 represents gross primary production, whereas it is generally agreed that over short incubation periods, the ^{14}C method measures something between net (gross production minus respiration) and gross production (STEEMAN NIELSEN, 1955). Thus any equation used to fit ^{14}C data should allow the possibility of a negative intercept. PLATT and JASSBY (1976) attempted to cater for this possibility by adding a constant to equation (5) which could be estimated from the data. They found in practice however that this constant was a small quantity with a large estimated error and so this technique was not very successful. One way round this problem would be to assume some definite value for the respiration rate, add this to the ^{14}C results and then use equation (5) to fit what would now be a gross production curve. STEEMAN NIELSEN and HANSEN (1959) reported 78 measurements of respiration made by extrapolating ^{14}C measurements to zero light level and the mean of these values was close to 10% of P_m. However, STEEMAN NIELSEN and HANSEN (1959) estimated that in a four hour experiment the respiration rate (as measured by the experiment) will only be 6% of P_m.

It is first necessary to obtain some preliminary estimate of P_m. This was done by fitting equation (5) to the uncorrected ^{14}C results and using the resulting values of α, β and P_s to calculate a rough value for P_m which will be called P'_m. If it is assumed that respiration was 6% of the true P_m then a better estimate for P_m will be given by $P''_m = P'_m/0.94$. The quantity $0.06P''_m$ was then added to the ^{14}C results to convert them to a gross production which was then fitted by equation (5) to obtain new estimates of α, β and P_s. If the resulting value of P_m was very different from the earlier estimate the process could be repeated, but in practice it was found that one iteration was adequate. The curve was fitted using a standard non-linear regression method (JENRICH and SAMPSON, 1968).

The values obtained by this method, with their standard errors, were $\alpha = 0.4 \pm 0.1$, $\beta = 0.008 \pm 0.006$, $P_s = 4.8 \pm 0.6$ mg C [mg chlorophyll a]$^{-1}$ hr^{-1}, and the resulting assimilation ratio P_m was 4.4. The estimated value of β was not significantly different from zero at the 5% level but as it is known *a priori* that phytoplankton are inhibited by strong light this term will be retained. In order to demonstrate the fit of the curve to the experimental data, the curve $P_g(I) - 0.06P_m$ using the estimated values of α, β, P_s and P_m has been plotted in Fig. 20.

The quantity $P_g - 0.1P_m$ gives the net primary production of carbon per unit chlorophyll concentration per unit time. It will be assumed that during the day the production rate of chlorophyll will be proportional to the net production of carbon and that the constant of proportionality is the inverse of the carbon-to-chlorophyll ratio γ. At night carbon is lost from cells by respiration. However, it is unlikely that this process will result in any significant loss of chlorophyll over periods of a few days and so it will be assumed that the growth rate of chlorophyll is zero when the net primary production is less than zero. This assumption differs from that made by JAMART, WINTER, BANSE, ANDERSON and LAM (1977) who were modelling longer term changes and made the simplifying assumption that γ did not change diurnally. As discussed below, when modelling short term changes, this assumption would

produce large diurnal fluctuations in the modelled chlorophyll concentration, which would not be consistent with field observations.

The carbon-to-chlorophyll ratio γ was assumed to be constant in the model. In reality this will not strictly be true due to photo-adaptation or changes in species composition which may take place during a spring bloom. However, in view of the very different estimates of γ obtained using the techniques discussed in Section 4.5, any more complicated parameterisation was not considered. It is also known from experiments with phytoplankton cultures (e.g. HUNTER and LAWS, 1981) that γ changes diurnally, due largely to the effects of photosynthesis and respiration on cell carbon levels, and tends to be lowest at the end of the dark period and highest at the end of the light period. The samples used to estimate the value of γ were spread evenly throughout the day and night and so should represent a mean value of these diurnal changes. This implies that the model will tend to underestimate γ in the morning and overestimate it in the afternoon and so over a twelve hour period these two errors will partly compensate each other.

Nutrient limitation of phytoplankton growth is represented in the model by multiplying the gross production by a Michaelis–Menten term. Thus the net primary production r in hr^{-1} is given by

$$r = \frac{(P_g - 0.1P_m)}{\gamma} \cdot \frac{N}{N + K_N} \tag{7}$$

where γ is the carbon to chlorophyll ratio and K_N the nutrient half-saturation constant. The quantity P_m in this equation and the related quantity P_s in equation (5) are now defined as the values that would be observed for non-limiting nitrate concentrations and these values along with K_N must now be estimated. This was done by using the production–irradiance curves for ^{14}C experiments 1 and 2, which showed the largest differences in P_m values. Due to the small number of observations it was not possible to fit equation (5) to the observations for a single experiment. Therefore, the P_m values were estimated by eye as 4.9 and 3.6 for experiments 1 and 2 respectively, with associated nitrate concentrations of 6 and 1 μM. The P_m values were then corrected for respiration as described previously and the Michaelis–Menten expression was used to give two simultaneous equations in K_N and the true P_m. This process gave a K_N of 0.6, P_m of 5.7 and using equation (6) a P_s of 6.3.

5.5.2. *The irradiance–depth curve.* The most commonly used parameterisation for the irradiance $I(z, t)$ is given by

$$I(z, t) = (1 - a)I_0(t) \exp\left(-k_1 z - k_c \int_0^z C(z, t)\mathrm{d}z\right) \tag{8}$$

where a is the albedo, $I_0(t)$ the surface irradiance, k_1 the attenuation coefficient for water and all material except plants and k_c the phytoplankton self-shading coefficient (WINTER, BANSE and ANDERSON, 1975). It was found however that this equation was inadequate for fitting the irradiance–depth curves obtained on this survey as it fails to take into account the well-known fact that blue–green light is much less readily absorbed than either longer (red) or shorter (violet) wavelengths (JERLOV, 1976). Thus the irradiance falls off rapidly just below the surface as the red and violet light is absorbed after which the irradiance decreases in a near-asymptotic exponential manner as the blue–green light is absorbed. Such a situation can be described by assuming that the irradiance is the sum of two exponential terms (PAULSON and SIMPSON, 1977) both of which will be modified by the absorption of plant material. The resulting equation for irradiance is then given by

$$I(z,t) = (1-a)I_0(t)(Re^{-k_1 z} + (1-R)e^{-k_2 z}) \exp\left(-k_c \int_0^z C(z,t)dz\right) \quad (9)$$

where k_2 is the attenuation coefficient for blue-green light, k_1 the absorption coefficient for the remainder and $1-R$ the fraction of blue-green light in the total spectrum. If k_1 is sufficiently greater than k_2 then it is possible to estimate all the parameters of equation (9), except a, from a depth profile of irradiance and chlorophyll (see Appendix C). Five such profiles were obtained at the end of Survey 2 (see Fig. 9) and four of these were used to estimate the parameters of equation (9). The mean values and standard errors were $R = 0.51 \pm 0.04$, $k_1 = 0.29 \pm 0.01\ m^{-1}$, $k_2 = 0.14 \pm 0.01\ m^{-1}$ and $k_c = 0.026 \pm 0.005\ m^2$ [mg chlorophyll a]$^{-1}$.

The values of k_1 and k_2 agree well with the data presented by JERLOV (1976) for the clearest coastal water (type I). The value of k_c is similar to that obtained by BANNISTER (1974) who took the mean of a number of independent experimental observations. An average albedo of 7% was assumed (PAYNE, 1972) as being typical of conditions for this latitude at this time of year. The incident photosynthetic irradiance $I_0(t)$ was calculated by multiplying the hourly values of incident total solar irradiance, measured at Aberporth, Wales (Fig. 5), by the conversion factor 0.4 (see Appendix A).

5.5.3. *Diffusion and phytoplankton sinking.* The diffusivities calculated in Section 5.3 (Fig. 27) were used as estimates of K_z. For deeper depths for which no estimate of K_z was available a constant diffusivity was assumed, equal to the mean of the two deepest K_z estimates. The method of estimating K_z produced some negative values in the thermocline region for position A between Surveys 2 and 3 (see Appendix B). For the model these were replaced by a value equal to the lowest observed positive value from that K_z profile. In between any two surveys K_z was assumed constant at a given depth but was allowed to take different values for the two time periods. This method of modelling the different degrees of wind mixing observed during the whole survey period is obviously over-simplified, but is the best that can be achieved without developing a more explicit model of the physical stratification.

No direct observations of phytoplankton sinking rates were made on the cruise. Instead the parameterisation suggested by JAMART, WINTER, BANSE, ANDERSON and LAM (1977) was used, which related sinking rate to the nutrient concentration in accordance with the observations of STEELE and YENTSCH (1960). A sinking rate v_0 and v_∞ is defined for zero and very high nutrient concentrations respectively and it is assumed that normally $v_0 > v_\infty$. The sinking rate in between these two values is determined by the nutrient concentration N and the parameter N^* in the following way

$$v = v_\infty \text{ for } N \geqslant 2N^*$$

$$v = v_0 + \tfrac{1}{2}(v_\infty - v_0)(N/N^*)^2 \text{ for } 0 \leqslant N \leqslant N^*$$

$$v = \tfrac{1}{2}(v_0 + v_\infty) - (v_0 - v_\infty)[(N-N^*)/N^*] + \tfrac{1}{2}(v_0 - v_\infty)[(N-N^*)/N^*]^2 \text{ for } N^* \leqslant N \leqslant 2N^*.$$

JAMART, WINTER, BANSE, ANDERSON and LAM (1977) used values of 2.5 μM, 2.5 m day^{-1} and 0.5 m day^{-1} for N^*, v_0 and v_∞ respectively and, in the absence of any other data, these values were used in most of the simulations described below but the sensitivity of the results to the parameter v_0 was investigated.

5.5.4. *Nutrient uptake and herbivore grazing.* The nutrient uptake was assumed to be proportional to net photosynthesis and a carbon to nitrate ratio of 5.7 was assumed (see Section 4.3).

The model of JAMART, WINTER, BANSE, ANDERSON and LAM (1977) assumed that this proportionality applied throughout 24 hours, which implied that nutrients would be regenerated when the net production was less than zero. There is very little evidence that this process takes place over short time periods and so we will follow RADACH (1980) and assume that no uptake takes place unless the net production is greater than zero.

A modified Michaelis–Menten expression was used to model the grazing rate for an individual herbivore as a function of plant carbon (RADACH, 1980). This quantity must then be multiplied by the density of herbivores to obtain the grazing term b of equation (4). In RADACH's (1980) model of the North Sea bloom the zooplankton term was not modelled explicitly but was obtained from field data. As no zooplankton data were obtained on our cruise this approach cannot be used. Instead we will assume that over the short time period of the three surveys the numbers of zooplankton will not change greatly and can be assumed to be constant. This assumption will not be correct for the protozooplankton (see Table 1) but is probably not unreasonable for copepods and other large zooplankton grazing on the diatoms. RADACH (1980) reports data obtained by KRAUSE on the concentration of copepods in the North Sea during the FLEX experiment and these show that the copepods do not start increasing in number significantly until about ten days after the start of the bloom.

If, therefore, we assume a constant herbivore density the grazing term as a function of chlorophyll concentration is given by

$$b = \frac{G(\gamma C - \epsilon)}{(\gamma C - \epsilon + K_g)}$$

where G is the maximum grazing rate ($\mathrm{mg\,C\,m^{-3}\,hr^{-1}}$), ϵ a grazing threshold and K_g a half-saturation contant. RADACH (1980) used the North Sea grazing experiments of GAMBLE (1978) to estimate the quantities ϵ and K_g and obtained values of 6.5 $\mathrm{mg\,C\,m^{-3}}$ and 11 $\mathrm{mg\,C\,m^{-3}}$ respectively. These values of K_g and ϵ were used in all the simulations reported below while the parameter G was treated as a free variable that could be adjusted to fit the model to observed data.

5.5.5. *Numerical methods.* Equations (4) were simulated using the Crank–Nicholson technique and the Thomas algorithm for solving the simultaneous equations at each time step (VON ROSENBERG, 1969). A number of trials were made using different values of the time step Δt and depth interval Δz. It was found that results of sufficient accuracy were obtained using $\Delta t = 1$ hr and $\Delta z = 0.5$ m. Zero flux boundary conditions were assumed for chlorophyll and nitrate at the water surface and at the bottom, and a water depth of 95 m was used for all simulations.

The initial chlorophyll profiles for positions A and B were those shown in Figs 24 and 25 for Survey 1 and the model was run for the period between the occupation of these stations on Surveys 1 and 2. Constant chlorophyll values were assumed for depths below the depth of undulator observations. The one nutrient–depth profile made on Survey 1 showed that the nitrate concentration was virtually the same at the surface and 70 m and so constant values of 5.5 and 6.25 $\mu\mathrm{M}^{-1}$ were used for the initial nitrate profiles at positions B and A respectively [see Fig. 6(b)].

5.6. *Model results*

5.6.1. *Development of the mixed layer phytoplankton bloom between Surveys 1 and 2.* Most of the parameters of the model described in the previous section have been estimated from data obtained on the cruise. This was not the case, however, with the grazing rate and the phytoplankton sinking rate. Furthermore the three methods used to estimate γ gave three very different values. There are therefore a number of model parameters that are either undetermined or uncertainly determined and this must be borne in mind when using the model.

Attention will first be focussed on the predicted chlorophyll and nitrate development at a depth of 2 m between Surveys 1 and 2 at position A and the first simulations show the effect of assuming different values of γ. The values of v_0, v_∞ and N^* were 2.5, 0.5 and 2.5 respectively and herbivore grazing was assumed for the moment to be zero. The results show (Fig. 29) that in all three cases there was an initial period of growth followed by a decline due to the onset of nutrient limitation. However, the magnitude and timing of the initial growth phase varies greatly with γ. For $\gamma = 17$ the phytoplankton initially grows rapidly reaching a peak of 24 mg m^{-3} chlorophyll *a* after only two days and this rapid growth reduces the nitrate concentration to very low levels. Thereafter there are small periods of growth at the beginning of each light period, produced by fresh nitrate diffusing upwards at night, but the general trend is downwards to a final chlorophyll value of 10.0 mg m^{-3}. It should be noted that chlorophyll concentrations as high as 24 mg m^{-3} have never been observed in the Celtic Sea in spring or in the central North Sea (HORWOOD, pers. comm.). For $\gamma = 45$ the chlorophyll reached a peak of 8.5 mg m^{-3} declining to 3.6 mg m^{-3} after $5\frac{1}{2}$ days, while for $\gamma = 63$ the curve peaked at 6 mg m^{-3} after 3 days declining to 2.8 mg m^{-3}. In all three cases the final predicted nitrate levels were much lower than the observed values (Fig. 9) and the predicted phytoplankton population was declining by Survey 2, whereas the observations showed that there was phytoplankton growth between Surveys 2 and 3. It is therefore necessary to reduce the rate at which nitrate is used up and this can be done by introducing some grazing pressure which will also reduce the unrealistically high chlorophyll values.

The effect of altering the grazing level on the simulated results for a γ value of 17 are shown in Fig. 30. The value of the parameters ϵ and K_g were 6.5 mg C m^{-3} and 11 mg C m^{-3} respectively,

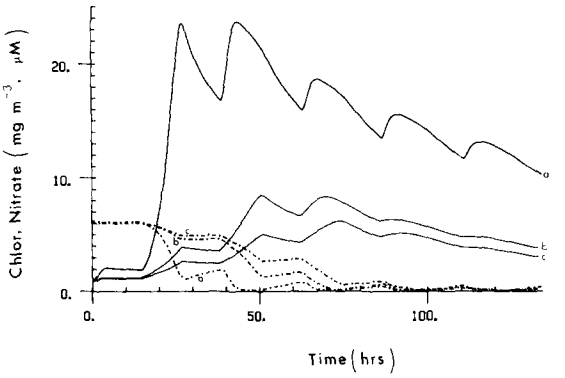

FIG. 29. Model results for changes in surface chlorophyll *a* (mg m^{-3}, solid lines) and nitrate (μM, dashed lines) concentrations at position A between Surveys 1 and 2, assuming no grazing by zooplankton. Three possible carbon to chlorophyll ratios (γ) are considered: (a) $\gamma = 17$; (b) $\gamma = 45$; (c) $\gamma = 63$.

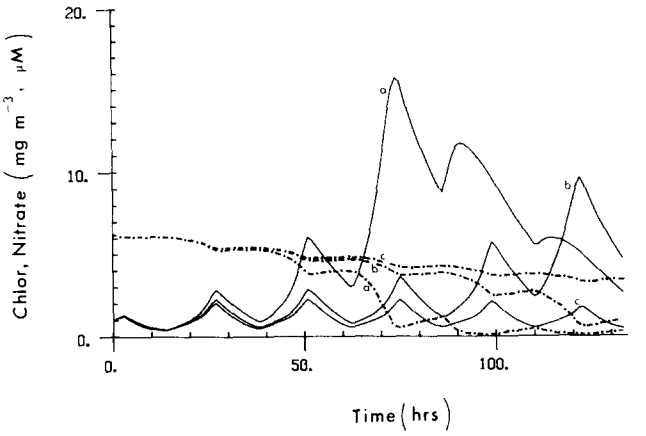

FIG. 30. Model results for changes in surface chlorophyll *a* (mg m^{-3}, solid lines) and nitrate (μM, dashed lines) concentration at position A between Surveys 1 and 2, assuming a carbon-to-chlorophyll ratio of 17. Three possible values of the grazing function, G, are considered: (a) $G = 4.0$; (b) $G = 4.5$; (c) $G = 4.75$.

while G took the values 4.0, 4.5 and 4.75 mg C m^{-3} hr^{-1}. The effect of grazing at these levels has been to control the large bloom that occurred in the first few days when no grazing was assumed. However, in the succeeding three days the phytoplankton development is quite different for the three cases. For $G = 4.0$ a bloom develops on the third day reaching levels of 15.5 mg m^{-3} and thereafter declining due to nutrient limitation. For $G = 4.75$ the phytoplankton growth is completely controlled by the grazing pressure and the chlorophyll never rises above 2 mg m^{-3} and the nitrate concentration remains above 3.5 μM. However for $G = 4.5$ the nitrate levels decline gradually over the 5½ days reaching a final value of 1 μM which is close to the observed values on Survey 2. The changeover between the situation with high and low nitrate concentrations at the end of 5½ days is critically dependent on the grazing pressure. In Fig. 31 the predicted chlorophyll and nitrate concentrations at the end of this time interval have been plotted against the parameter G. This plot shows that the model switches from one state to the other between 4 and 4.5 mg C m^{-3} hr^{-1} and that in this region the predicted chlorophyll value can be

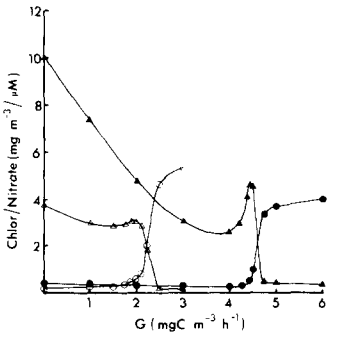

FIG. 31. Model results for surface chlorophyll *a* (mg m^{-3}, triangles) and nitrate (μM, circles) concentrations at position A at the time of Survey 2, as a function of grazing coefficient G assuming a carbon-to-chlorophyll ratio of 17 (closed symbols) and 45 (open symbols).

actually higher than that for slightly lower grazing levels. This sensitivity of the model to the value of G may be heightened by the assumption of constant grazing pressure and it could be that a more realistic model which included a specific zooplankton term would show a more gradual change between the nutrient controlled and grazing controlled situations.

Another factor that is not taken into account by the model is nutrient regeneration by zooplankton. This would be in the form of ammonium or urea which could be taken up preferentially by the phytoplankton thus conserving nitrate nutrients. Thus if this process had been included in the model it would not require such a high grazing rate in order to obtain the nitrate concentration observed on Survey 2. However despite these limitations the model results demonstrate that it is necessary to assume a reasonably high level of grazing between Surveys 1 and 2, otherwise nutrient levels are reduced to such low levels that no further growth is possible between Surveys 2 and 3.

So far attention has been concentrated on the final predicted values at the end of the $5\frac{1}{2}$ days between Surveys 1 and 2. However Fig. 30 shows that, for $\gamma = 17$ and $G = 4.5$, there are substantial diurnal changes in chlorophyll caused by the joint effect of downward diffusion and grazing at night when no chlorophyll synthesis is taking place. On the final day of the simulation the chlorophyll reaches a peak of $10\,\mathrm{mg\,m^{-3}}$ declining to $4.3\,\mathrm{mg\,m^{-3}}$ by the end of the simulated period. A number of simulations were made varying the parameters ϵ and K_N to test whether the diurnal variations were sensitive to these parameters. It was found that by setting ϵ to zero, that is no threshold on herbivore grazing, the grazing level required to control the bloom could be reduced. Using $G = 2$ the predicted chlorophyll and nitrate concentrations were $8.6\,\mathrm{mg\,m^{-3}}$ and $0.8\,\mu\mathrm{M}$ respectively. However, the diurnal variations for this run were just as large as those shown in Fig. 30.

The assumption of a γ value of 17 thus presents a dilemma. If low levels of grazing are assumed the resulting high net growth rate produces chlorophyll levels in the first few days that are higher than observed in the field and also reduces the nitrate to very low levels. However, if the grazing role is increased to bring this initial bloom under control, the required level of grazing produces diurnal variations in chlorophyll which are, again, not observed in the field. It was therefore decided to investigate the effects of grazing for a γ value of 45. The results of these simulations are summarised in Fig. 31 and they show that only half the grazing pressure is required to control the bloom development compared to the results for $\gamma = 17$. Furthermore the diurnal range of chlorophyll (Fig. 32) is only 20% of the maximum daily value which is a more acceptable figure than the 50% obtained for $\gamma = 17$. However, the predicted chlorophyll level after $5\frac{1}{2}$ days was only $2.8\,\mathrm{mg\,m^{-3}}$ which is less than half the observed value on Survey 2 (Fig. 24). A closer agreement with the observations can be obtained by varying v_0 the phytoplankton sinking rate at low nutrient concentrations. The effect of this parameter on the predicted chlorophyll and nitrate levels is shown in Table 2 for γ equal to 17 and 45. In both cases decreasing v_0 increases the final chlorophyll value without greatly affecting the nitrate levels. The simulated results for $\gamma = 45$ and $v_0 = 0.5\,\mathrm{m\,day^{-1}}$ (Fig. 32) yields a final chlorophyll concentration of $4.8\,\mathrm{mg\,m^{-3}}$ which is however still less than the observed value.

These results demonstrate that it is possible to produce simulations of the mixed layer bloom that are in reasonable agreement with the observations. However in order to achieve this it was necessary to use a γ value of 45 and also to assume values for grazing rate and phytoplankton sinking rates which cannot be confirmed or rejected from the data obtained on the cruise. These results show how important it is to obtain measurements of these parameters before reliable attempts can be made to model the spring bloom development.

However, it is worth noting that, for the grazing coefficient, G, to have a significant effect on

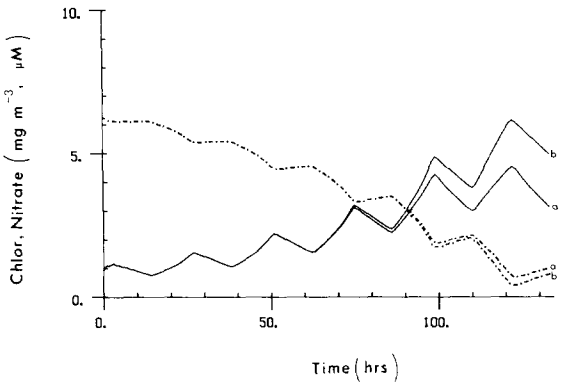

FIG. 32. Model results for changes in surface chlorophyll *a* ($mg\,m^{-3}$, solid lines) and nitrate (μM, dashed lines) concentrations at position A between Surveys 1 and 2, assuming a carbon-to-chlorophyll ratio of 45. Two values for the phytoplankton sinking rate at low nutrient concentrations (v_0) are considered:
(a) $v_0 = 2\,m\,day^{-1}$; (b) $v_0 = 0.5\,m\,day^{-1}$.

TABLE 2. EFFECT OF THE SINKING RATE PARAMETER v_0 ON THE PREDICTED CHLOROPHYLL AND NITRATE CONCENTRATION AT THE END OF A $5\frac{1}{2}$ DAY PERIOD. THE CHLOROPHYLL CONCENTRATION ($mg\,m^{-3}$) IS THE FIRST OF THE PAIR OF FIGURES AND THE NITRATE CONCENTRATION (μM) THE SECOND.

v_0 ($m\,day^{-1}$)	2.5	2.0	1.5	1.0	0.5
$\gamma = 17$ $G = 4.5$	4.2, 1.0	4.8, 0.9	5.5, 0.9	6.2, 0.8	6.9, 0.8
$\gamma = 45$ $G = 2.1$	2.8, 1.0	3.3, 0.9	3.7, 0.8	4.2, 0.8	4.8, 0.8

the development of the phytoplankton population, maximum grazing rates in the range 1–2 $g\,C\,m^{-2}\,day^{-1}$ are implied. These are typical of values estimated from the FLEX data (DARO, 1980). Another important feature of the grazing response is the time difference between the increase in phytoplankton and increase in the various groups of herbivores. It is apparent from information of zooplankton succession in the spring (e.g. HARVEY, 1950) and from comparable data on phyto- and zoo-plankton abundance (e.g. KRAUSE and RADACH, 1980) that groups such as copepod nauplii and the larvae of benthic organisms become significantly more abundant at the same time as, or even before, the diatom peak. Thus in assuming G to be constant over $5\frac{1}{2}$ days, grazing may have been overestimated at the beginning and underestimated at the end. This effect appears not to have been important during the FLEX work in the North Sea when the increase in grazing was largely a response to the increase in food (DARO, 1980), but in the Celtic Sea where *Calanus* is a less dominant herbivore and protozooplankton appear to be relatively abundant (Table 1) this assumption needs to be further investigated.

So far the simulations have been limited to position A. At position B the calculated eddy diffusivities were higher than at A and the net phytoplankton growth between Surveys 1 and 2 was much less (Fig. 25). A series of runs were made to test the effect of grazing on phytoplankton growth at B and the results are summarised in Fig. 33. A comparison of this figure with

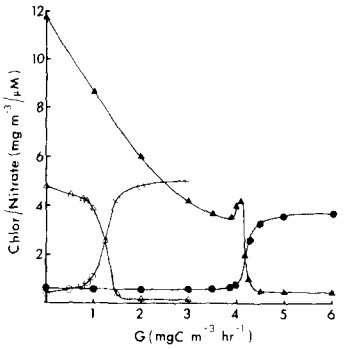

FIG. 33. Model results for surface chlorophyll a (mg m^{-3}, triangles) and nitrate (μM, circles) concentrations at position B at the time of Survey 2 as a function of grazing rate coefficient G, assuming carbon-to-chlorophyll ratios of 17 (closed symbols) and 45 (open symbols).

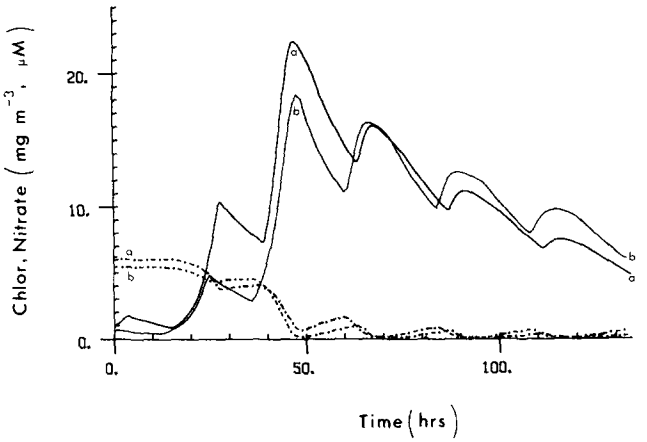

FIG. 34. Model results for changes in surface chlorophyll a (mg m^{-3}, solid lines) and nitrate (μM, dashed lines) concentration between Surveys 1 and 2, assuming values of 2.0 and 17 respectively for the grazing function, G, and the carbon-to-chlorophyll ratio, γ, at (a) position A and (b) position B.

Fig. 31 shows that for low G the predicted chlorophyll level after $5\frac{1}{2}$ days is actually higher at B than at A. The reason for this is demonstrated by Fig. 34 which shows the bloom development at A and B for $G = 2.0\,\text{mg C m}^{-3}\text{hr}^{-1}$. The phytoplankton growth over the first two days is less at B than A due to the high turbulent diffusion at B. However, in the succeeding 3 days when growth is nutrient limited, the higher diffusion rates at B result in slightly more nitrate being diffused up from below the thermocline at night, resulting in higher final chlorophyll values.

At very high grazing rates the predicted values at B are the same as for A. However, the change from the nutrient controlled to the grazing controlled situation occurs at a much lower grazing rate at B than at A, and this may provide the clue to the differences between the bloom development at these two positions. Thus assuming a γ of 45 a grazing rate of $2\,\text{mg C m}^{-3}\text{hr}^{-1}$ would yield a $5\frac{1}{2}$ day chlorophyll value of $2.8\,\text{mg m}^{-3}$ at A but only $0.2\,\text{mg m}^{-3}$ at B. These values can be modified by assuming different values of v_0 as described above, but the results

demonstrate the possibility that a given grazing rate might allow the bloom to develop at position A but not at position B. In the absence of any field estimates of grazing pressure this explanation of the differences between phytoplankton growth at A and B must be treated as speculative.

5.6.2. *Development of the chlorocline between Surveys 1 and 2.* One of the surprising features of the bloom development between Surveys 1 and 2 was that, before the increase in wind speed during the latter part of Survey 2, the chlorocline was consistently 10 m below the thermocline (Fig. 24). In Fig. 35 the simulated depth distribution of chlorophyll $5\frac{1}{2}$ days after Survey 1 is shown for various values of the model parameters. Two profiles are from runs already described from the previous section for γ values of 17 and 45. When these profiles are compared with the observed profile (Fig. 24) it is clear that the model completely fails to reproduce the deep chlorocline. Instead the model chlorocline is at the same depth as the observed thermocline. It was found that adjusting the sinking rate parameters in various ways had only a small effect on the chlorophyll distribution in the thermocline region. For example, if the values of v_0 and v_∞ were altered from 0.5 and 0.5 m day^{-1} respectively to 1.0 and 0.0 m day^{-1}, then for $\gamma = 45$ the chlorophyll at 10 m only increased from 1 to 1.7 mg m^{-3}.

This failure to reproduce the deep chlorocline is due to the fact that the photosynthesis parameters used in the model yield a daily averaged compensation depth of between 18 and 20 m, so that the modelled growth rate between 15 and 20 m was very low. This fact combined with the effects of grazing means that the model phytoplankton growth below the thermocline is insufficient to counteract the increased turbulent diffusion in the region (Fig. 27). This point can best be appreciated by comparing the time scales for diffusion and phytoplankton growth at different depths calculated using the model (Table 3). The diffusive time scale was calculated by introducing a population of non-growing phytoplankton into the appropriate depth zone and using the model to estimate the time taken for the population in the middle of the zone to be reduced by one half. The growth time scales were calculated by running the model for one day assuming no diffusion or sinking. The net growth rate r was then calculated for a depth in the middle of the zone and a time scale from $0.693/r$ (the time for the population to double at that growth rate). Growth time scales were calculated for $\gamma = 17$ and 45 and for both zero grazing and grazing rates G of 4.5 and 2.1 g C m^{-3} hr^{-1} respectively.

The diffusive time scale in the top 5 m is 40 hr and this is longer than the time scale of

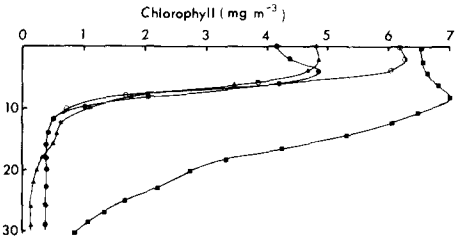

FIG. 35. Model results for profiles of chlorophyll a (mg m^{-3}) at position A at the time of Survey 2 using the following values for model parameters (see text for explanation of symbols).
○—○ $\gamma = 17$, $G = 4.5$, $v_0 = 1.0$, $v_\infty = 0.5$
●—● $\gamma = 17$, $G = 4.5$, $v_0 = 2.5$, $v_\infty = 0.5$
▲—▲ $\gamma = 45$, $G = 2.1$, $v_0 = 0.5$, $v_\infty = 0.5$
■—■ observed data.

TABLE 3. TIME SCALES FOR DIFFUSION AND PHYTOPLANKTON GROWTH IN THE DEPTH ZONES 0–5 m AND 5–10 m

Depth zone (m)	Diffusive time scale (hr)	Growth, time scale (with grazing) (hr)		Growth, time scale (without grazing) (hr)	
		$\gamma = 17, G = 4.5$	$\gamma = 45, G = 2.1$	$\gamma = 17$	$\gamma = 45$
0–5	40	14	41	6	23
5–10	12	17	336	9	38

phytoplankton growth with grazing for $\gamma = 17$ (23 hr) and of the same order as that for $\gamma = 45$ (41 hr). This is as expected as the simulations have shown that for these values of G and γ the population in surface mixed layer will grow. However, the diffusive time scale in the thermocline region between 5 and 10 m, is 12 hr and this is considerably shorter than the time scales of growth with grazing time scales for either γ value implying that, in the model, diffusive processes will dominate in the region as was indeed found to be the case (Fig. 35). It is interesting to note that the growth without grazing time scale for $\gamma = 17$ was 9 hr and so for this γ value an ungrazed phytoplankton population would be able to maintain itself in the thermocline region. However, it is difficult to imagine why this region should be immune from zooplankton grazing although the grazing at this depth might be less than in the top 5 m. Another mechanism whereby net growth could be higher in the thermocline region is photo-adaptation. MARRA (1980) has shown that the physiological response time of a diatom *Lauderia borealis* to an eightfold decrease in light levels was ten hours which is of the same order as the diffusive time scale in the thermocline. Furthermore PERRY, LARSEN and ALBERTE (1981) have reported a fourfold increase in photosynthetic efficiency per photosynthetic unit when cultures of phytoplankton were grown at low light levels. It is possible, therefore, that a combination of photo-adaptation plus reduced grazing levels might be able to explain the development of the deep chlorocline.

Another possibility is that the eddy diffusivity has been overestimated in the thermocline. PINGREE, PUGH, HOLLIGAN and FORSTER (1975) reported a thermocline time scale of a week compared to our estimate of 12 hr. However, their estimate was calculated from the warming of the bottom mixed layer over the spring–summer period, when the mean temperature difference across the thermocline is much greater than over the period of our three surveys. However, it should be remembered that the estimates of eddy diffusivity, obtained by the method described in Section 5.3, were average values for the whole $5\frac{1}{2}$ day period between Surveys 1 and 2. It has already been mentioned that, in reality, the diffusivities will be changing with time, and that at the beginning of the period when stratification is still minimal, the diffusivity in the thermocline region will be less than the average value, thus perhaps allowing phytoplankton growth to take place at this time.

It is clear that the ability to reproduce the development of the deep chlorocline provides a critical test of a phytoplankton model, and until this feature can be satisfactorily modelled no attempt can be made to try and understand other interesting features of the chlorophyll depth distribution such as the persistance of the sub-surface peaks (Fig. 17).

5.6.3. *Development of the surface phytoplankton between Surveys 2 and 3.* In the last two sections it was shown that, by an appropriate choice of parameters, the model was able, to some extent, to explain the development of the phytoplankton bloom in the surface waters,

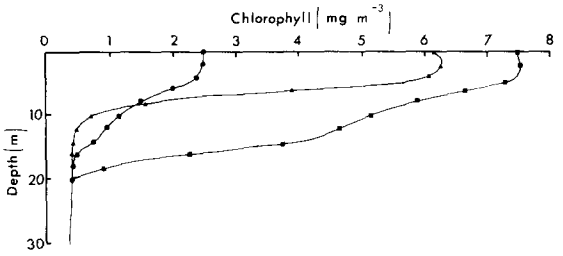

FIG. 36. Model results for profiles of chlorophyll *a* (mg m^{-3}) at position A, assuming a value of 17 for the carbon-to-chlorophyll ratio, at the time of (a) Survey 2, grazing function $G = 4.5$, ▲; (b) Survey 3, $G = 4.5$, ●; (c) Survey 3, $G = 4.5$ between Survey 1 and 2 and $G = 2.0$ between Surveys 2 and 3, ■.

but that it could not explain the development of a chlorocline below the thermocline. In view of this failure any attempt to extend the modelling exercise from Survey 2 to Survey 3 should be treated with caution and only two simulations will be reported here. Both these simulations assumed $\gamma = 17$ and $v_0 = 1.0$ m day^{-1} while the parameters v_∞, N^*, ϵ, K_g and K_N were as quoted at the beginning of Section 5.6.1. For the first $5\frac{1}{2}$ days a grazing rate G of 4.5 mg C m^{-3}hr^{-1} was assumed and the resulting chlorophyll profile is shown in Fig. 36. At this point in the simulation the diffusion coefficients were changed to those calculated for the Survey 2 to 3 period (Fig. 27) and the simulation run for a further two days. If the grazing rate was kept unchanged, it was found that the increased vertical mixing, between the surface and 15 m, produced by this change in eddy diffusivities caused a sharp reduction in the chlorophyll concentration in the top 10 m, although between 10 m and 15 m the chlorophyll increased due to the deepening of the thermocline. The observations at position A (Fig. 24) showed that in fact the surface chlorophyll concentration increased between Surveys 1 and 2 from 6.5 mg m^{-3} to 8 mg m^{-3}. If the new eddy diffusivities are assumed to be correct, and if the value of γ has not altered, then it is necessary to reduce the level of grazing in order to bring the model results in line with the observations. It was found that if G was reduced from 4.5 to 2.0 mg C m^{-3}hr^{-1} for the last 2 days of the simulation then the surface chlorophyll increased from 6.2 to 7.5 mg m^{-3} over this period, while the nitrate concentration remained virtually unchanged. The vertical profiles for this run (Fig. 36) show that the predicted chlorocline has deepened by about 10 m, however, it is still not as deep as the observed chlorocline on Survey 3 (Fig. 24). These results further demonstrate that we have some way to go before being able to predict the vertical structure of chlorophyll in the spring bloom.

Two possible reasons may be postulated for the necessity of reducing the grazing pressure for the last two days of the simulation. Firstly the increased mixing will tend to disperse the microzooplankton in the same way as the phytoplankton which must reduce the grazing pressure in the surface layers to some extent. Secondly, in the model the change in mixing regions was introduced instantaneously whereas in reality this change would take place more slowly giving time for more phytoplankton growth than predicted by the model.

6. DISCUSSION

In the northern Celtic Sea, a region with relatively weak tides, the main development of the spring diatom outburst is controlled by the formation of the seasonal thermocline. The timing of these events appears, from direct observations (PINGREE, 1975; PINGREE, HOLLIGAN,

MARDELL and HEAD, 1976; this investigation) and from physical models (JAMES, 1977), to be relatively consistent from year to year within the constraints of spring to neap tidal cycles and prevailing weather conditions. Once a vertical density gradient corresponding to a surface to bottom temperature difference $> 0.2°C$ has become established, levels of chlorophyll *a* and particulate material increase rapidly to reach a maximum within 5–10 days with a marked depletion of dissolved inorganic nutrients. The time scale for comparable changes in the northern North Sea during FLEX (WEICHART, 1980; GIESKES and KRAAY, 1980) was similar, and is probably typical for the spring bloom in deeper (> 70 m) shelf waters that become stratified during April.

However, both from field observations and by implication from our modelling experiments, it is apparent that significant variations do occur in the rate of development of the spring bloom over horizontal scales of the order of 50 km, and in the relative importance of nutrients and grazing in limiting the standing stock of phytoplankton. The ways in which environmental factors can interact to cause these variations are still poorly understood and the subject of considerable speculation, but the attempt to model the diatom outburst in the Celtic Sea for a period of a few days has focussed attention on certain aspects of this problem which are usually overlooked in longer term, low resolution models (e.g. HORWOOD, 1982).

Before the thermocline is formed in the Celtic Sea, surface chlorophyll *a* values are generally in the range 0.5–1.0 mg m^{-3} and significantly higher than the minimum winter levels of about 0.2 mg m^{-1} (PINGREE, HOLLIGAN, MARDELL and HEAD, 1976). This initial increase in the standing stock of phytoplankton, is presumed to be related to increases in light and perhaps short-lived periods of stratification during the early spring, and is likely to be important in enabling certain groups of zooplankton to produce eggs and juvenile developmental stages before the main phase of phytoplankton growth. As yet there are no data on zooplankton populations in the Celtic Sea to support this hypothesis, but the high grazing rates suggested by the model could be explicable in these terms.

Once the water column is stratified, the observed initial increases in the standing stock of phytoplankton in the surface mixed layer can be adequately modelled in terms of light and nutrient availability, as determined by the depth of the thermocline, vertical eddy diffusivity, and grazing. It appears that these three parameters largely account for the main temporal (e.g. at position A) and spatial (e.g. between positions A and B) variations in phytoplankton abundance at this time of year. Similar patchiness in the distribution of chlorophyll in the spring has been described from the North Sea by STEELE and HENDERSON (1979). Although some of the other parameters used in the model equations may not have been accurately evaluated, it is clear that estimates of phytoplankton carbon (i.e. carbon to chlorophyll ratios) and herbivore grazing rates are the most uncertain terms. In a dynamic sense, these are closely interrelated. Either, as we have suggested, phytoplankton carbon is a relatively small proportion of total POC, inferring a high specific growth rate with the rapid production of non-phytoplankton carbon; or, at the opposite extreme, levels of phytoplankton carbon are high and rates of primary and secondary production relatively low.

To distinguish between these two situations, compatible data on the abundance and activity of the herbivores including protozooplankton (Table 1) are required. Other lines of evidence are also relevant. Marked diel changes in phytoplankton carbon to chlorophyll or particulate carbon to nitrogen ratios due to respiratory losses of carbon should be detectable in rapidly growing populations. The observation of DARO (1980) from the FLEX data that consistent decreases in particulate carbon levels at night could not be entirely explained by grazing, give some support for this hypothesis. In situations where losses of phytoplankton due to sinking

and grazing are minimal, the changes in concentrations of chlorophyll *a* and dissolved nutrients provide some information about the carbon to chlorophyll ratio, as long as the elemental composition of the plant cells approximates to the Redfield ratio (see GOLDMAN, MCCARTHY and PEAVEY, 1979). Thus, the high chlorophyll levels (> 30 mg m^{-3}) relative to phosphorus uptake in Loch Creran (TETT, COTTRELL, TREW and WOOD, 1975) and to nitrate uptake in the Norwegian coastal current (DAHL and DANIELSSEN, 1981) during March are consistent with low carbon to chlorophyll ratios. When grazing is important, diel changes in chlorophyll levels should also be apparent. But for marine diatom populations there appear to be no well documented cases of this effect, probably because of the difficulties in sampling organisms that generally show uneven spatial distributions.

An important indicator of control of the phytoplankton population by grazing may be the degree of nitrate depletion. In this study, as well as in the FLEX data, nitrate concentrations declined to about 1 μM which is still a relatively high level compared to surface values in mid-summer ($< 0.2\,\mu$M), and to the half saturation constant for nitrate uptake by phytoplankton. The model results reported here suggest that it is necessary to postulate a high grazing rate from the early stages of the spring bloom in order to prevent the surface nutrient concentrations being reduced to very low levels within a few days of the start of the bloom. Furthermore, with a high grazing rate, regenerated forms of nitrogen, such as NH_4 and urea which are assimilated more readily than NO_3, would become available as the bloom developed thus further limiting the depletion of nitrate. However, it is also important to note that in 1975 (PINGREE, HOLLIGAN, MARDELL and HEAD, 1976) and 1980 (unpublished observations), the surface nitrate concentrations in the Celtic Sea were $\sim 0.1\,\mu$M by the end of April. Consideration of Figs 31 and 33 leads to the hypothesis that the grazing pressure may have been a little lower in these years, at least initially, so that the nitrate was depleted more quickly.

A second fundamental problem concerns the depths of the chlorocline and the formation of subsurface chlorophyll maxima. The attempts to model the chlorocline suggested that basic information, about changes with depth in photosynthetic–irradiance relationships and in the carbon to chlorophyll ratio, and also about possible variations in the phytoplankton sinking rate in relation to nutrient status of the cells, is required before any realistic explanation of the vertical distribution of chlorophyll can be put forward. This applies especially to the later stages of the diatom bloom (i.e. Survey 3) when the discrepancies between the field observations and the model predictions were greatest. These difficulties may stem partly from the method used to calculate eddy diffusion across the pycnocline, so in the future the modelling of physical mixing processes will have to be improved perhaps by using the techniques of JAMES (1977).

The results of the observational programme reported in this paper demonstrate the important insights that can be obtained about the temporal and spatial development of the spring bloom using high resolution undulator surveys. The important points to emerge are that significant differences in the spring bloom development can take place over space scales of 50 km and that between depths of 5 to 15 m the phytoplankton population shows a remarkable degree of independence of the turbulent diffusive processes. Furthermore the attempts at modelling the observed changes in the surface mixed layer show that it is necessary to postulate a high degree of grazing from the start of the bloom. The attempts to model the phytoplankton growth in the 5 to 15 m region were unsuccessful and further research into the reasons for this might repay considerable dividends in our understanding of the dynamics of the spring diatom bloom. A number of possible alterations and extensions of the model that might improve its predictive power in the thermocline region are, the addition of photo-adaptation and nutrient regeneration and the improvement of the parameterisation of eddy diffusivity.

Acknowledgements–We would like to acknowledge the help of the officers and crew of R.R.S. Challenger in carrying out the three surveys reported here. We would also acknowledge the considerable technical support provided by the staff of the N.E.R.C. Shipboard Computer Group and of the Applied Physics and Engineering groups at I.O.S., with especial mention of the help provided by John Burnham, John Smithers and Vincent Lawford and to Bob Head (M.B.A.) for carrying out the chemical analyses. We would also wish to thank Ian Vassie for calculating the tidal velocities and Robin Pingree for making available the results of his calculations of the stratification parameter and Derek Harbour for counting the phytoplankton samples.

REFERENCES

BANNISTER, T. T. (1974) A general theory of steady state phytoplankton growth in a nutrient saturated mixed layer. *Limnology and Oceanography*, **19**, 13–30.

BANSE, K. (1977) Determining the carbon-to-chlorophyll ratio of natural phytoplankton. *Marine Biology*, **41**, 199–212.

BOWDEN, K. F. (1955) Physical oceanography of the Irish Sea. *Fishery Investigations*, Series II, **18**, No. 8, 67 pp.

COOPER, L. H. N. (1960) Some theorems and procedures in shallow-water oceanography applied to the Celtic Sea. *Journal of the Marine Biological Association of the United Kingdom*, **39**, 155–171.

COOPER, L. H. N. (1961) The oceanography of the Celtic Sea II. Conditions in the spring of 1950. *Journal of the Marine Biological Association of the United Kingdom*, **41**, 235–270.

CULLEN, J. J. and E. H. RENGER (1979) Continuous measurement of the DCMU-induced fluorescence response of natural phytoplankton. *Marine Biology*, **53**, 13–20.

DAHL, E. and D. S. DANIELSSEN (1981) Hydrography, nutrient and phytoplankton in the Skagerrak along the section Torungen–Hirtshals, January–June 1980. In: *The Norwegian Coastal Current*, R. SAETRE and M. MORK, editors, University of Bergen, 294–310.

DARO, M. H. (1980) Field study of the diel feeding of a population of *Calanus finmarchicus* at the end of a phytoplankton bloom. *"Meteor" Forschungsergebnisse*, Reihe A, No. 22, 123–132.

EPPLEY, R. W. (1972) Temperature and phytoplankton growth in the sea. *Fishery Bulletin*, **70**, 1063–1085.

EPPLEY, R. W., W. G. HARRISON, S. W. CHISHOLM and E. STEWART (1977) Particulate organic matter in surface waters off Southern California and its relationship to phytoplankton. *Journal of Marine Research*, **35**, 671–696.

EPPLEY, R. W., F. M. H. REID and J. D. H. STRICKLAND (1970) Estimates of phytoplankton crop size, growth rate and primary production. In: *The ecology of the plankton off La Jolla, California in the period April through September, 1967*, Vol. 17, J. D. H. STRICKLAND, editor. Bulletin Scripps Institution of Oceanography, pp. 33–42.

FASHAM, M. J. R., P. R. PUGH, D. GRIFFITHS and J. E. G. WHEATON (1981) Subaquatraka: a submersible fluorimeter for the detection of chlorophyll. In: *Electronics for Ocean Technology*, proceedings of a conference held at Birmingham, 8–10th September, 1981, Institution of Electronic and Radio Engineers, pp. 49–58.

FRIEHE, C. A. and K. F. SCHMITT (1976) Parameterization of air–sea interface fluxes of sensible heat and moisture by the bulk aerodynamic formulas. *Journal of Physical Oceanography*, **6**, 801–809.

GAMBLE, J. C. (1978) Copepod grazing during a declining spring phytoplankton bloom in the northern North Sea. *Marine Biology*, **49**, 303–315.

GIESKES, W. W. C. and G. W. KRAAY (1980) Primary productivity and phytoplankton pigment measurements in the northern North Sea during FLEX '76. *"Meteor" Forschungsergebnisse*, Reihe A, No. 22, 105–112.

GOLDMAN, J. C., J. J. MCCARTHY and D. G. PEAVEY (1979) Growth rate influence on the chemical composition of phytoplankton in oceanic waters. *Nature, London*, **279**, 210–215.

HARTREE, D. R. (1958) *Numerical analysis*, The Clarendon Press, 302 pp.

HARVEY, H. W. (1950) On the production of living matter in the sea off Plymouth. *Journal of the Marine Biological Association of the United Kingdom*, **29**, 97–137.

HOLM-HANSEN, O., C. J. LORENZEN, R. W. HOLMES and J. D. H. STRICKLAND (1965) Fluorometric determination of chlorophyll. *Journal du Conseil*, **30**, 3–15.

HORWOOD, J. (1982) Algal production in the west-central North Sea. *Journal of Plankton Research*, **4**, 103–124.

HUNTER, B. L. and E. A. LAWS (1981) ATP and chlorophyll *a* as estimators of phytoplankton carbon biomass. *Limnology and Oceanography*, **26**, 944–956.

JAMART, B. M., D. F. WINTER, K. BANSE, G. C. ANDERSON and R. K. LAM (1977) A theoretical study of phytoplankton growth and nutrient distribution in the Pacific Ocean off the northwestern U.S. coast. *Deep-Sea Research*, **24**, 753–773.

JAMES, I. D. (1977) A model of the annual cycle of temperature in a frontal region of the Celtic Sea. *Estuarine and Coastal Marine Science*, **5**, 339–353.

JAMES, I. D. (1980) Thermocline formation in the Celtic Sea. *Estuarine and Coastal Marine Science*, **10**, 597–607.

JASSBY, A. and T. POWELL (1975) Vertical patterns of eddy diffusion during stratification in Castle Lake, California. *Limnology and Oceanography*, **20**, 530–543.

JEFFREY, K. G., E. M. GILL, R. T. POLLARD and D. S. COLLINS (1977) *G-EXEC system user's manual.* Natural Environment Research Council, United Kingdom.

JENNRICH, R. I. and P. F. SAMPSON (1968) Application of stepwise regression to nonlinear least squares estimation. *Technometrics*, **10**, 63–78.

JERLOV, N. G. (1976) *Marine Optics*, Elsevier Scientific Publishing Company, 231 pp.

KAHN, D. A., P. R. PUGH, M. J. R. FASHAM and M. J. HARRIS (1975) Underwater logarithmic irradiance meter for primary production and associated studies; In: *Instrumentation in Oceanography*, proceedings of a conference held at Bangor, Wales on the 23rd–25th September 1975, Institution of Electronic and Radio Engineers, pp. 81–90.

KIEFER, D. A. (1973) Chlorophyll *a* fluorescence in marine centric diatoms: responses of chloroplasts to light and nutrient stress. *Marine Biology*, **23**, 39–46.

KRAUSE, M. and G. RADACH (1980) On the succession of developmental stages of herbivorous zooplankton in the northern North Sea during FLEX '76. First statements about the main groups of the zooplankton community. *"Meteor" Forschungsergebnisse*, Reihe A, No. 22, 133–150.

MARRA, J. (1980) Time course of light intensity adaptations in a marine diatom. *Marine Biology Letters*, **1**, 175–183.

MILLARD, R. A., J. TOOLE and M. SWARTZ (1980) A fast responding temperature measurement system for CTD applications. *Ocean Engineering*, **7**, 413–427.

NEUMANN, G. and W. J. PIERSON (1966) *Principles of physical oceanography*, Prentice-Hall, 545 pp.

PAULSON, C. A. and J. J. SIMPSON (1977) Irradiance measurements in the upper ocean. *Journal of Physical Oceanography*, **7**, 952–956.

PAYNE, R. E. (1972) Albedo of the sea surface. *Journal of Atmospheric Sciences*, **29**, 959–970.

PERRY, M. J., M. C. LARSEN and R. S. ALBERTE (1981) Photoadaptation in marine phytoplankton: response of the photosynthetic unit. *Marine Biology*, **62**, 91–101.

PINGREE, R. D. (1975) The advance and retreat of the thermocline on the continental shelf. *Journal of the Marine Biological Association of the United Kingdom*, **55**, 965–974.

PINGREE, R. D. and D. K. GRIFFITHS (1978) Tidal fronts on the shelf seas around the British Isles. *Journal of Geophysical Research*, (Oceans and atmosphere), Chapman Conference special issue, **83**, 4615–4622.

PINGREE, R. D. and D. K. GRIFFITHS (1980) Currents driven by a steady uniform wind stress on the shelf seas around the British Isles. *Oceanologica Acta*, **3**, 227–236.

PINGREE, R. D., P. M. HOLLIGAN, G. T. MARDELL and R. N. HEAD (1976) The influence of physical stability on spring, summer and autumn phytoplankton blooms in the Celtic Sea. *Journal of the Marine Biological Association of the United Kingdom*, **56**, 845–873.

PINGREE, R. D., P. R. PUGH, P. R. HOLLIGAN and G. R. FORSTER (1975) Summer phytoplankton blooms and red tides along tidal fronts in the approaches to the English Channel. *Nature, London*, **258**, 672–677.

PLATT, T., K. L. DENMAN and A. D. JASSBY (1977) Modelling the productivity of phytoplankton. In: *The Sea*, Vol. 6, E. D. GOLDBERG, I. N. MCCAVE, J. J. O'BRIEN and J. H. STEELE, editors, Wiley-Interscience, pp. 807–856.

PLATT, T., C. L. GALLEGOS and W. G. HARRISON (1980) Photoinhibition of photosynthesis in natural assemblages of marine phytoplankton. *Journal of Marine Research*, **38**, 687–701.

PLATT, T. and A. D. JASSBY (1976) The relationship between photosynthesis and light for natural assemblages of coastal marine phytoplankton. *Journal of Phycology*, **12**, 421–430.

POLLARD, R. T. (1980) Reduction of JASIN batfish data. *JASIN News*, No. 17, 10–11.

RADACH, G. (1980) Preliminary simulations of the phytoplankton and phosphate dynamics during FLEX '76 with a simple two-component model. *"Meteor" Forschungsergebnisse*, Reihe A, No. 22, 151–164.

SAMPSON, R. J., (1978) *SURFACE II graphics system (version one).* Kansas Geological Survey, 240 pp.

SIMPSON, J. H. , D. G. HUGHES and N. C. G. MORRIS (1977) The relation of seasonal stratification to tidal mixing on the continental shelf. In: *A voyage of discovery*, M. V. ANGEL, editor, Pergamon Press, pp. 327–340.

SLOVACEK, R. E. and P. J. HANNAN (1977) *In vivo* fluorescence determinations of phytoplankton chlorophyll *a*. *Limnology and Oceanography*, **22**, 919–925.

SMITH, R. C. (1969) An underwater spectral irradiance collector. *Journal of Marine Research*, **27**, 341–351.

STEELE, J. H. and I. E. BAIRD (1962) Carbon–chlorophyll relations in cultures. *Limnology and Oceanography*, **7**, 101–102.

STEELE, J. H. and E. W. HENDERSON (1979) Spatial patterns in North Sea plankton. *Deep-Sea Research*, **26**, 955–963.
STEELE, J. H. and C. S. YENTSCH (1960) The vertical distribution of chlorophyll. *Journal of the Marine Biological Association of the United Kingdom*, **39**, 217–226.
STEEMAN NIELSEN, E. (1955) The interaction of photosynthesis and respiration and its importance for the determination of ^{14}C discrimination in photosynthesis. *Physiologia Plantarum*, **8**, 945–953.
STEEMAN NIELSEN E. and V. HANSEN (1959) Measurements with the carbon-14 technique of the rates of respiration in natural populations of phytoplankton. *Deep-Sea Research*, **5**, 222–233.
STRICKLAND, J. D. H. (1968) Continuous measurement of *in vivo* chlorophyll: a precautionary note. *Deep-Sea Reseach*, **15**, 225–227.
STRICKLAND, J. D. H. and T. R. PARSONS (1968) *A practical handbook of seawater analysis*. Fisheries Research Board of Canada, 311 pp.
TETT, P., J. C. COTTRELL, D. O. TREW and B. J. B. WOOD (1975) Phosphorus quota and the chlorophyll: carbon ratio in marine phyroplankton. *Limnology and Oceanography*, **20**, 587–603.
VON ROSENBERG, D. U. (1969) *Methods for the numerical solution of partial differential equations*. American Elsevier Publishing Company, 128 pp.
WEICHART, G. (1980) Chemical changes and primary production in the Fladen Ground area (North Sea) during the first phase of a spring phytoplankton bloom. "*Meteor*" *Forschungsergebnisse*, Reihe A, No. 22, 79–86.
WINTER, D. F., F. BANSE and G. C. ANDERSON (1975) The dynamics of phytoplankton blooms in Puget Sound, a fjord in the northwestern United States. *Marine Biology*, **29**, 139–176.
WROBLEWSKI, J. S. (1977) A model of phytoplankton plume formation during variable Oregon upwelling. *Journal of Marine Research*, **35**, 357–394.
YORKE, D. (1966) Least-squares fitting of a straight line. *Canadian Journal of Physics*, **44**, 1079–1086.

APPENDIX A
CALCULATION OF THE NET HEAT FLUX INTO THE WATER COLUMN

The net heat flux (Q) (calories cm^{-2} min^{-1}) from the atmosphere to the water column can be calculated from the formula (NEUMANN and PIERSON, 1966; JAMES, 1977):

$$Q = Q_s(1-a) - Q_\ell - Q_e - Q_h \tag{A1}$$

where Q_s is the total solar radiation, a the albedo, Q_ℓ the net heat loss from the sea due to long wave radiation, Q_e the evaporative heat flux and Q_h the sensible heat flux. Q_e was calculated from the formula

$$Q_e = 1.3 \times 10^{-3} \rho_a w(q_s - q_a)L \tag{A2}$$

(FRIEHE and SCHMITT, 1966) where w is the wind speed at 10 m ($m\,s^{-1}$), q_s the saturation specific humidity near the sea surface, q_a the specific humidity at 10 m, ρ_a the air density and L the latent heat of evaporation. Specific humidity q is given by

$$q = 0.622e/(p - 0.378e) \tag{A3}$$

where e is the vapour pressure and p the air pressure. The sensible heat flux was calculated from

$$Q_h = 1.3 \times 10^{-3} w C_a(T_s - T_a) \tag{A4}$$

(FRIEHE and SCHMITT, 1976) where C_a is the specific heat of air, T_s the sea surface and T_a the air temperature (°C).

The net heat loss from the sea due to long wave radiation is a function of the cloudiness and sea surface temperature. The heat loss per minute was calculated from the formula

$$Q_\ell = a_t(0.12 + 1.2 \times 10^{-3} T_s - 7 \times 10^{-5} T_s^2)/0.75, \tag{A5}$$

(P. M. SAUNDERS, personal communication) where a_t is the atmospheric transmittance. a_t is calculated from the ratio of the observed daily total of solar radiation to the theoretical value calculated from the date and latitude of the survey area. An albedo of 7% was used, derived

TABLE 4. COMPARISON OF PHOTOSYNTHETIC SOLAR IRRADIANCE MEASURED ON THE SHIP AND TOTAL SOLAR IRRADIANCE MEASURED AT THE ABERPORTH OBSERVATORY MEASURED IN WATT-HOURS m^{-2}

Date	Photosynthetic irradiance Q_p	Total solar irradiance Q_s	Q_p/Q_s
12/4	28.6	62.3	0.46
13/4	45.2	112.0	0.40
14/4	74.5	218.3	0.34
15/4	37.4	239.4	0.16
16/4	57.8	219.3	0.26
17/4	57.7	267.4	0.22
18/4	94.0	221.7	0.42
19/4	34.7	68.8	0.50
20/4	99.4	263.8	0.38
21/4	73.9	178.1	0.41

from the climatological values quoted by PAYNE (1972) for the appropriate latitude and month. During the cruise, observations of solar radiation were only made in the wavelength range 350–700 nm. However observations of total solar radiation for this period have been obtained from the Aberporth Observatory in south-west Wales which is about 90 miles from the survey area. In Table 4 the total daily solar radiation at Aberporth is compared with the total photosynthetic radiation recorded on the ship. On the 12th, 13th and 18th–21st of April, when the ship was in the survey area, the ratio is reasonably constant, while on the intervening days, when the ship was working some hundred miles to the west of the area, the ratio is different and more variable. This implies that the cloud cover at Aberporth and in the survey area was very similar on the days when the ship was in the area and it will be assumed that this was also true from the 14th–17th of April.

For the period between Surveys 2 and 3 values of T_s at positions A and B at four-hourly intervals were determined by linear interpolations between the observed values on these surveys. These values together with the four-hourly values of w, e, p and T_a recorded on the ship and the Aberporth Q_s values were used to estimate four hourly integrated values of Q_e, Q_ℓ and Q_h. Finally these values were added to obtain the total heat input Q for that period.

Between Surveys 1 and 2 the ship was not in the survey area and so the values of w, e, p and T_a were obtained if possible from meteorological reports from other ships in the area. If no ship's data were available for a given period then estimates for w, p and T_a were obtained by averaging the observations from the meteorological stations at Hartland Point, England and Roche's Point, Ireland. The survey area lay about halfway across the Celtic Sea on a direct line between these two stations and over this period the time series of these variables was very similar at both places. This method could not be used to estimate the vapour pressure e as the land–sea difference for this variable is likely to be too great. In this case therefore a value of e from the nearest ship's observation was used.

The average values of the variables making up equation (A1) are given in Table 5 for position A and B over the time intervals between Surveys 1 and 2 and Surveys 2 and 3. The heat input to the sea Q ranges from 51% to 61% of the incident radiation Q_s with most of the heat loss being due to the re-radiated long wave radiation.

TABLE 5. AVERAGE VALUES OF QUANTITIES INVOLVED IN THE CALCULATION OF OF HEAT INPUT TO THE SEA. ALL HEAT FLUXES ARE MEASURED IN Cal cm^{-2} day^{-1}

Time Period	Time Interval (hrs)	Position	Q_s	Q_e	Q_h	Q_ℓ	Q	Q/Q_s
Survey 1 to 2	134	A	437.3	2.7	−15.2	150.8	268.5	0.61
Survey 1 to 2	134	B	433.4	9.3	− 9.5	149.7	253.6	0.59
Survey 2 to 3	48	A	344.6	30.0	−15.0	116.0	189.0	0.55
Survey 2 to 3	48	B	342.3	36.5	−12.0	118.0	176.0	0.51

APPENDIX B
CALCULATION OF EDDY DIFFUSIVITIES

The equation used to calculate the eddy diffusivity K_z at depth Z is

$$\frac{\mathrm{d}}{\mathrm{d}t}\int_Z^{Z_m} T(u,t)\,\mathrm{d}u = -K_z\frac{\partial T}{\partial Z} - F + R_z/\rho C, \tag{B1}$$

where $T(u, t)$ is the temperature at depth u and time t, Z_m the average depth of the bottom of the undulator cycles, F the downwards heat flux from Z_m, R_z the flux of solar radiation at depth z and ρ, C are the density and specific heat of sea water (JASSBY and POWELL, 1975). The left-hand side of equation (B1) was calculated from the average temperature profiles (Figs 24, 25) for two given surveys and the time difference between them. The quantity $\partial T/\partial z$, which must be evaluated at the depth z, was calculated by estimating the first differential from the first and second temperature profiles, using a second order central difference formula (HARTREE, 1958), and then using the mean of the two values.

The quantity R_z is calculated from

$$R_z = Q\sum_{i=1}^{3} a_i\, e^{-k_i z} \tag{B2}$$

where Q is the net solar irradiance input to the water at the surface (as defined in Appendix A), a_i is the fraction of that radiation in the ith band and k_i the attenuation coefficient for that band. The three bands consist of two in the visible range (i = 1, 2) and the third in the infra-red, Average values of k_1 and k_2 were derived from underwater irradiance observations made on the cruise (see Appendix C), while k_3 was assumed equal to $2\,m^{-1}$ (NEUMANN and PIERSON, 1966). The proportion of visible to total solar radiation was calculated using the data from Table 4 of Appendix A, using the first three and last four days only, which yielded a figure of 0.4. It was then assumed (see Appendix A, Table 5) that the only loss of the visible light was caused by reflection at the sea surface which means that:

$$a_1 + a_2 = \frac{0.4(1-a)Q_s}{Q} \tag{B3}$$

where the quantities a, Q_s and Q are defined in Appendix A. Finally a_1 and a_2 were determined separately using the ratio $R = a_1/(a_1 + a_2)$ where R is derived in Appendix C.

The quantity F can be determined by substituting $z = 0$ in equation (B1) and assuming that $\partial T/\partial Z = 0$ at the surface which yields

$$F = Q/\rho C - \frac{\mathrm{d}}{\mathrm{d}t}\int_0^{z_m} T(u,t)\,\mathrm{d}u \tag{B4}$$

All the quantities in equation (B1) have now been defined and K_z can be calculated at 1 m intervals for all depths except the top and bottom of the temperature profile where $\partial T/\partial z$ cannot be estimated. The calculations for Position A for the time period between Surveys 2 and 3 gave some very small negative values for K_z in the region at the base of the thermocline. The true eddy diffusivity in this region is presumably extremely small and the negative values are the result of random variation about this small value. At Position B the calculations of K_z were only made down to a depth of 30 m as below this depth the temperature was isothermal.

APPENDIX C
ESTIMATION OF THE PARAMETERS OF THE IRRADIANCE–DEPTH RELATIONSHIP

Five profiles of underwater irradiance and chlorophyll *a* fluorescence were made on the 20th of April, one each at the western end of legs 32, 34, 36, 38 and 40 (see Table 6 for details). The average atmospheric transmittance on this day was 12%. Each profile was from 3 m to 60 m and took about 4 minutes to complete. The top 3 m were not sampled due to logistic reasons. The raw one second data were calibrated, sorted on pressure to combine down and up profiles, and then averaged over 1 m depth bands. The profile of log-irradiance for dip 3 (Fig. 37) clearly shows the change in the rate of light attenuation with depth caused by the preferential absorption of red and violet light.

The equation to be fitted to the irradiance data is

$$I_z = (1-a)I_0(R_e^{-k_1 z} + (1-R)e^{-k_2 z}) \exp\left(-k_c\int_0^z C(z)\,\mathrm{d}z\right) \tag{C1}$$

which is the equation suggested by PAULSON and SIMPSON (1977) modified to include the absorption of phytoplankton. I_0 is the incident irradiance at the sea surface, a the albedo, $C(z)$ the chlorophyll *a* concentration in mg m^{-3} and k_1, k_2, k_c and R are all constants which must be estimated. The values of a were estimated from sun altitude and atmospheric transmittance using the data of PAYNE (1972). The sun altitude for dip 5 was very low which makes the estimation of a from Payne's data rather dubious.

Before estimating k_1 or k_2, k_c must first be estimated. It is easy to show that

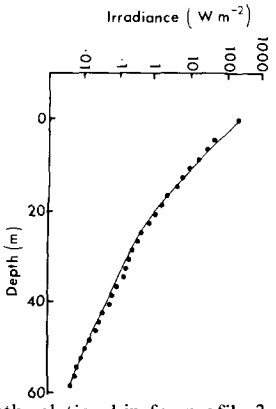

FIG. 37. Observed irradience–depth relationship for profile 3 (•) with theoretical curve fitted using equation C1.

$$\frac{d(\ln(I_z))}{dz} = F(z) - k_c C(z) \tag{C2}$$

where $F(z)$ is a function of z, k_1, k_2 and R. Thus k_c can be determined from the regressions of the differential on C. The differential was estimated from the 1 metre values of $\ln(I_z)$ using a second order centred-difference formula (HARTREE, 1958) and the regression was calculated using the major axis regression method of YORKE (1966). The values of k_c obtained are given in Table 6 together with the correlation coefficient between C and the differential $d(\ln(I_z))/dz$. Except for dip 1 the correlation coefficient was about 0.6 which is significant at the 0.1% level.

The next step was to estimate k_2 and R using the deeper part of the irradiance curve which represents the absorption of blue–green light only. If we define the quantity

$$A_z = \exp\left(-k_c \int_0^z C(z)\,dz\right)$$

then the equation for the deep section of the curve will be

$$\ln(I_z) = \ln((1-a)I_0) + \ln(A_z) + \ln(1-R) - k_2 z \tag{C3}$$

and the parameters k_2 and R can be determined from the standard regression of the quantity $\ln(I_z/A_z)$ on z. It is of course necessary to define the depth below which this calculation should be made. PAULSON and SIMPSON (1977) used 10 m, a choice partly necessitated by the small number of their observations. This depth would obviously be wrong for the present data and as observations have been made every metre, it was decided to err on the side of caution and so a depth of 40 m was chosen.

In order to estimate k_1 from the shallow part of the curve the quantity

$$Y_z = I_z/[(1-a)I_0 A_z] - (1-R)\,e^{-k_2 z}$$

was calculated for the shallow part of the curve. k_1 can then be determined from the regression of $\ln(Y_z)$ on z. For this purpose only values in the top 10 m were used, including the value $Y_0 = R$.

The estimated value for all the parameters and their standard errors are given in Table 6. The high value of $1-a$ for dip 5 resulted in a nonsensical value for R of less than zero, which meant that k_1 could not be estimated for this dip. This run was therefore discarded and average values of the parameters were obtained using the first four dips only.

TABLE 6. ESTIMATED VALUES OF THE PARAMETERS OF THE IRRADIANCE–DEPTH RELATIONSHIP. SEE TEXT FOR DEFINITION OF SYMBOLS

Dip No	Time of Day (GMT)	Sun Altitude	$1-a$	R	k_1 m^{-1}	k_2 m^{-1}	k_c m^2 (mg chlorophyll a)$^{-1}$	Correlation between $\frac{d/\ln(I_z)}{\partial z}$ and $C(z)$
1	1101–1145	49°	0.96	0.65 ± 0.07	0.30 ± 0.06	0.178 ± 0.007	0.043 ± 0.006	0.14
2	1321–1336	46°	0.96	0.47 ± 0.07	0.29 ± 0.10	0.137 ± 0.002	0.019 ± 0.004	0.59
3	1518–1520	33°	0.93	0.42 ± 0.07	0.32 ± 0.03	0.123 ± 0.004	0.018 ± 0.004	0.58
4	1652–1659	18°	0.85	0.48 ± 0.05	0.25 ± 0.09	0.110 ± 0.002	0.023 ± 0.004	0.61
5	1833–1846	4°	0.63	–	–	0.100 ± 0.002	0.031 ± 0.006	0.59
Average of Dips 1–4			–	0.51 ± 0.04	0.29 ± 0.01	0.14 ± 0.01	0.026 ± 0.005	–